

Multivariate Output Analysis for Markov Chain Monte Carlo

Dootika Vats
Department of Statistics
University of Warwick
D.Vats@warwick.ac.uk

James M. Flegal *
Department of Statistics
University of California, Riverside
jfflegal@ucr.edu

Galina L. Jones †
School of Statistics
University of Minnesota
galin@umn.edu

October 2, 2017

Abstract

Markov chain Monte Carlo (MCMC) produces a correlated sample for estimating expectations with respect to a target distribution. A fundamental question is when should sampling stop so that we have good estimates of the desired quantities? The key to answering this question lies in assessing the Monte Carlo error through a multivariate Markov chain central limit theorem (CLT). The multivariate nature of this Monte Carlo error largely has been ignored in the MCMC literature. We present a multivariate framework for terminating simulation in MCMC. We define a multivariate effective sample size, estimating which requires strongly consistent estimators of the covariance matrix in the Markov chain CLT; a property we show for the multivariate batch means estimator. We then provide a lower bound on the number of minimum effective samples required for a desired level of precision. This lower bound depends on the problem only in the dimension of the expectation being estimated, and not on the underlying stochastic process. This result is obtained by

*Research supported by the National Science Foundation.

†Research supported by the National Institutes of Health and the National Science Foundation.

drawing a connection between terminating simulation via effective sample size and terminating simulation using a relative standard deviation fixed-volume sequential stopping rule; which we demonstrate is an asymptotically valid procedure. The finite sample properties of the proposed method are demonstrated in a variety of examples.

1 Introduction

Markov chain Monte Carlo (MCMC) algorithms are used to estimate expectations with respect to a probability distribution when independent sampling is difficult. Typically, interest is in estimating a vector of quantities. However, analysis of MCMC output routinely focuses on inference about complicated joint distributions only through their marginals. This, despite the fact that the assumption of independence across components holds only rarely in settings where MCMC is relevant. Thus standard univariate convergence diagnostics, sequential stopping rules for termination, effective sample size definitions, and confidence intervals all lead to an incomplete understanding of the estimation process. We overcome the drawbacks of univariate analysis by developing a methodological framework for multivariate analysis of MCMC output.

Let F be a distribution with support \mathcal{X} and $g : \mathcal{X} \rightarrow \mathbb{R}^p$ be an F -integrable function such that $\theta := E_F g$ is of interest. If $\{X_t\}$ is an F -invariant Harris recurrent Markov chain, set $\{Y_t\} = \{g(X_t)\}$ and estimate θ with $\theta_n = n^{-1} \sum_{t=1}^n Y_t$ since $\theta_n \rightarrow \theta$, with probability 1, as $n \rightarrow \infty$. Finite sampling leads to an unknown *Monte Carlo error*, $\theta_n - \theta$, estimating which is essential to assessing the quality of estimation. If for $\delta > 0$, g has $2 + \delta$ moments under F and $\{X_t\}$ is polynomially ergodic of order $m > (2 + \delta)/\delta$, an approximate sampling distribution for the Monte Carlo error is available via a Markov chain central limit theorem (CLT). That is, there exists a $p \times p$ positive definite matrix, Σ , such that as $n \rightarrow \infty$,

$$\sqrt{n}(\theta_n - \theta) \xrightarrow{d} N_p(0, \Sigma). \quad (1)$$

Thus the CLT describes asymptotic behavior of the Monte Carlo error and the strong law for θ_n ensures that large n leads to a small Monte Carlo error. But, how large is large enough? This question has not been adequately addressed in the literature since current approaches are based on the univariate CLT

$$\sqrt{n}(\theta_{n,i} - \theta_i) \xrightarrow{d} N(0, \sigma_i^2) \text{ as } n \rightarrow \infty, \quad (2)$$

where $\theta_{n,i}$ and θ_i are the i th components of θ_n and θ respectively and σ_i^2 is the i th diagonal element of Σ . Notice that a univariate approach ignores cross-correlation across components, leading to an inaccurate understanding of the estimation process.

Many output analysis tools that rely on (2) have been developed for MCMC (see Atchadé (2011), Atchadé (2016), Flegal and Jones (2010), Flegal and Gong (2015), Gelman and Rubin (1992), Gong and Flegal (2016), and Jones et al. (2006)). To determine termination, Jones et al. (2006) implemented the *fixed-width sequential stopping rule* where simulation is terminated the first time the width of the confidence interval for each component is small. More formally, for a desired tolerance of ϵ_i for component i , the rule terminates simulation the first time after some $n^* \geq 0$ iterations, for all components

$$t_* \frac{\sigma_{n,i}}{\sqrt{n}} + n^{-1} \leq \epsilon_i,$$

where $\sigma_{n,i}^2$ is a strongly consistent estimator of σ_i^2 , and t_* is an appropriate t -distribution quantile. The role of n^* is to ensure a minimum simulation effort (as defined by the user) so as to avoid poor initial estimates of σ_i^2 . This rule laid the foundation for termination based on quality of estimation rather than convergence of the Markov chain. As a consequence, estimation is reliable in the sense that if the procedure is repeated again, the estimates will not be vastly different (Flegal et al., 2008). However, implementing the fixed-width sequential stopping rule can be challenging since (a) careful analysis is required for choosing ϵ_i for each $\theta_{n,i}$ which can be tedious or even impossible for large p ;

(b) to ensure the right coverage probability, t_* is chosen to account for multiple confidence intervals (often by using a Bonferroni correction). Thus when p is even moderately large, these termination rules can be aggressively conservative leading to delayed termination; (c) simulation stops when each component satisfies the termination criterion; therefore, all cross-correlations are ignored and termination is governed by the slowest mixing components; and (d) it ignores correlation in the target distribution.

To overcome the drawbacks of the fixed-width sequential stopping rule, we propose the *relative standard deviation fixed-volume sequential stopping rule* that differs from the Jones et al. (2006) procedure in two fundamental ways; (a) it is motivated by the multivariate CLT in (1) and not by the univariate CLT in (2); and (b) it terminates simulation not by the absolute size of the confidence region, but by its size relative to the inherent variability in the problem. Specifically, simulation stops when the Monte Carlo standard error is small compared to the variability in the target distribution. Naturally, an estimate of the Monte Carlo standard error is required and for now, we assume that Σ can be estimated consistently. Later we will discuss procedures for estimating Σ . The relative standard deviation fixed-volume sequential stopping rule terminates the first time after some user-specified $n^* \geq 0$ iterations

$$\text{Volume of Confidence Region}^{1/p} + n^{-1} < \epsilon |\Lambda_n|^{1/2p}, \quad (3)$$

where Λ_n is the sample covariance matrix, $|\cdot|$ denotes determinant, and ϵ is the tolerance level. As in the univariate setting, the role of n^* is to avoid premature termination due to early bad estimates of Σ or Λ ; we will say more about how to choose n^* in Section 3.

Wilks (1932) defines the determinant of a covariance matrix as the *generalized variance*. Thus, an equivalent interpretation of (3) is that simulation is terminated when the generalized variance of the Monte Carlo error is small relative to the generalized variance of g with respect to F ; that is, a scaled estimate of $|\Sigma|$ is small compared to

the estimate of $|\Lambda| = |\text{Var}_F(Y_1)|$. We call $|\Lambda|^{1/2p}$ the *relative metric*. For $p = 1$, our choice of the relative metric reduces (3) to the relative standard deviation fixed-width sequential stopping rule of Flegal and Gong (2015).

We show that if the estimator for Σ is strongly consistent, the stopping rule in (3) is asymptotically valid, in that the confidence regions created at termination have the right coverage probability as $\epsilon \rightarrow 0$. Our result of asymptotic validity holds for a wide variety of relative metrics. A different choice of the relative metric, leads to a fundamentally different approach to termination. For example, if instead of choosing $|\Lambda|^{1/2p}$ as the relative metric, we choose a positive constant, then our work provides a multivariate generalization of the absolute-precision procedure considered by Jones et al. (2006).

Another standard way of terminating simulation is to stop when the number of effective samples for each component reaches a pre-specified lower bound (see Atkinson et al. (2008), Drummond et al. (2006), Giordano et al. (2015), Gong and Flegal (2016), and Kruschke (2014) for a few examples). We focus on a multivariate study of effective sample size (ESS) since univariate treatment of ESS ignores cross-correlations across components, thus painting an inaccurate picture of the quality of the sample. To the best of our knowledge, a multivariate approach to ESS has not been studied in the literature. We define

$$\text{ESS} = n \left(\frac{|\Lambda|}{|\Sigma|} \right)^{1/p}.$$

When there is no correlation in the Markov chain, $\Sigma = \Lambda$ and $\text{ESS} = n$. Notice that our definition of ESS involves the ratio of generalized variances. This ratio also occurs in (3) which helps us arrive at a key result; terminating according to the relative standard deviation fixed-volume sequential stopping rule is asymptotically equivalent to terminating when the estimated ESS satisfies

$$\widehat{\text{ESS}} \geq W_{p,\alpha,\epsilon},$$

where $W_{p,\alpha,\epsilon}$ can be calculated *a priori* and is a function only of the dimension of the estimation problem, the level of confidence of the confidence regions, and the relative precision desired. Thus, not only do we show that terminating via ESS is a valid procedure, we also provide a theoretically valid, practical lower bound on the number of effective samples required.

Recall that we require a strongly consistent estimator of Σ . Estimating Σ is a difficult problem due to the serial correlation in the Markov chain. Vats et al. (2017) demonstrated strong consistency for a class of multivariate spectral variance estimators while Dai and Jones (2017) introduced multivariate initial sequence estimators and established their asymptotic validity. However, both estimators are expensive to calculate and do not scale well with either p or n . Instead, we use the *multivariate batch means* (mBM) estimator of Σ which is significantly faster to compute (see Section 6) and requires weaker moment conditions on g for strong consistency. Our strong consistency result weakens the conditions required in Jones et al. (2006) for the univariate batch means (uBM) estimator. In particular, we do not require a one-step minorization and only require polynomial ergodicity (as opposed to geometric ergodicity). The condition is fairly weak since often the existence of the Markov chain CLT itself is demonstrated via polynomial ergodicity or a stronger result (see Jones (2004) for a review). Many Markov chains used in practice have been shown to be at least polynomially ergodic. See Acosta et al. (2015), Doss and Hobert (2010), Hobert and Geyer (1998), Jarner and Roberts (2002), Jarner and Hansen (2000), Jarner and Roberts (2002), Johnson et al. (2013), Johnson and Jones (2015), Jones et al. (2014), Jones and Hobert (2004), Khare and Hobert (2013), Marchev and Hobert (2004) Roberts and Polson (1994), Tan et al. (2013), Tan and Hobert (2012), Vats (2016), among many others.

The multivariate stopping rules terminate earlier than univariate methods since (a) termination is dictated by the joint behavior of the components of the Markov chain and not by the component that mixes the slowest (b) using the inherent multivariate

nature of the problem and acknowledging cross-correlations leads to a more realistic understanding of the estimation process, and (c) avoiding corrections for multiple testing give considerably smaller confidence regions even in moderate p problems. There are also cases where univariate methods *cannot* be implemented due to large memory requirements. On the other hand, the multivariate methods are inexpensive relative to the sampling time for the Markov chain and terminate significantly earlier. We present one such example in Section 5.4 through a Bayesian dynamic spatial-temporal model.

The rest of the paper is organized as follows. In the sequel we present a motivating Bayesian logistic regression model. In Section 2 we formally introduce a general class of relative fixed-volume sequential termination rules. In Section 3 we define ESS and provide a lower bound on the number of effective samples required for simulation. Our theoretical results in these sections require a strongly consistent estimator for Σ ; a result we show for the mBM estimator in Section 4. In Section 5 we continue our implementation of the Bayesian logistic regression model and consider additional examples. We choose a vector autoregressive process of order 1, where the convergence rate of the process can be manipulated. Specifically, we construct the process in such a way that one component mixes slowly, while the others are fairly well behaved. Such behavior is often seen in hierarchical models with priors on the variance components. The next example is that of a Bayesian lasso where the posterior is in 51 dimensions. We also implement our output analysis methods for a fairly complicated Bayesian dynamic spatial temporal model. For this example we do not know if our assumptions on the process hold, thus demonstrating the situation users often find themselves in. We conclude with a discussion in Section 6.

1.1 An Illustrative Example

For $i = 1, \dots, K$, let Y_i be a binary response variable and $X_i = (x_{i1}, x_{i2}, \dots, x_{i5})$ be the observed predictors for the i th observation. Assume τ^2 is known,

$$Y_i|X_i, \beta \stackrel{ind}{\sim} \text{Bernoulli}\left(\frac{1}{1 + e^{-X_i\beta}}\right), \quad \text{and} \quad \beta \sim N_5(0, \tau^2 I_5). \quad (4)$$

This simple hierarchical model results in an intractable posterior, F on \mathbb{R}^5 . The dataset used is the `logit` dataset in the `mcmc` R package. The goal is to estimate the posterior mean of β , $E_F\beta$. Thus g here is the identity function mapping to \mathbb{R}^5 . We implement a random walk Metropolis-Hastings algorithm with a multivariate normal proposal distribution $N_5(\cdot, 0.35^2 I_5)$ where I_5 is the 5×5 identity matrix and the 0.35 scaling approximates the optimal acceptance probability suggested by Roberts et al. (1997).

We calculate the Monte Carlo estimate for $E_F\beta$ from an MCMC sample of size 10^5 . The starting value for β is a random draw from the prior distribution. We use the mBM estimator described in Section 4 to estimate Σ . We also implement the uBM methods described in Jones et al. (2006) to estimate σ_i^2 , which captures the autocorrelation in each component while ignoring the cross-correlation. This cross-correlation is often significant as seen in Figure 1a, and can only be captured by multivariate methods like mBM. In Figure 1b we present 90% confidence regions created using mBM and uBM estimators for β_1 and β_3 (for the purpose of this figure, we set $p = 2$). This figure illustrates why multivariate methods are likely to outperform univariate methods. The confidence ellipse is the smallest volume region for a particular level of confidence. Thus, these confidence ellipses are likely to be preferred over other confidence regions.

To assess the confidence regions, we verify their coverage probabilities over 1000 independent replications with Monte Carlo sample sizes in $\{10^4, 10^5, 10^6\}$. Since the true posterior mean is unknown, we use $(0.5706, 0.7516, 1.0559, 0.4517, 0.6545)$ obtained by averaging over 10^9 iterations as a proxy. For each of the 1000 replications, it was noted whether the confidence region contained the true posterior mean. The volume of the confidence region to the p th root was also observed. Table 1 summarizes the results. Note that though the uncorrected univariate methods produce the smallest confidence

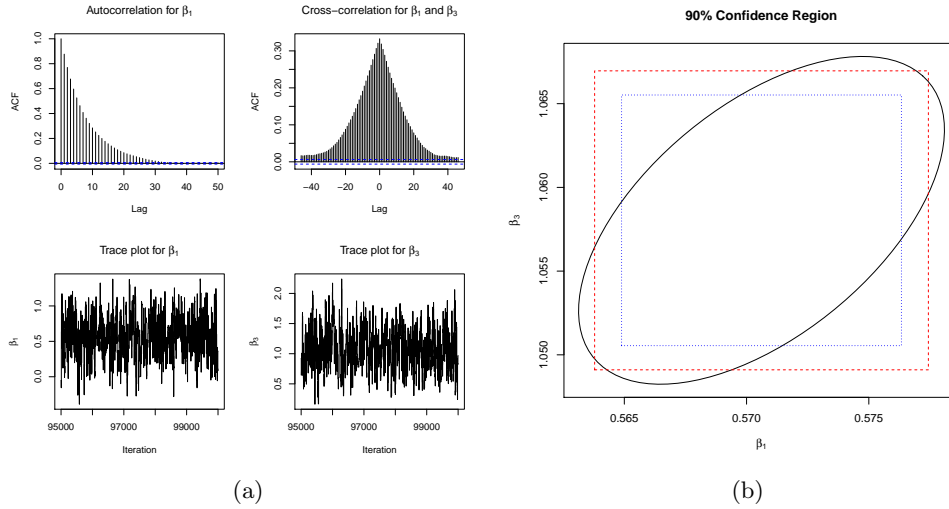


Figure 1: (a) ACF plot for β_1 , cross-correlation plot between β_1 and β_3 , and trace plots for β_1 and β_3 . (b) Joint 90% confidence region for β_1 and β_3 . The ellipse is made using mBM, the dotted line using uncorrected uBM, and the dashed line using the uBM corrected by Bonferroni. The Monte Carlo sample size is 10^5 for both plots.

regions, their coverage probabilities are far from desirable. For a large enough Monte Carlo sample size, mBM produces 90% coverage probabilities with systematically lower volume than uBM corrected with Bonferroni (uBM-Bonferroni).

Table 1: Volume to the p th ($p = 5$) root and coverage probabilities for 90% confidence regions constructed using mBM, uBM uncorrected, and uBM corrected by Bonferroni. Replications = 1000 and standard errors are indicated in parenthesis.

n	mBM	uBM-Bonferroni	uBM
Volume to the p th root			
1e4	0.062 (7.94e-05)	0.066 (9.23e-05)	0.046 (6.48e-05)
1e5	0.020 (1.20e-05)	0.021 (1.42e-05)	0.015 (1.00e-05)
1e6	0.006 (1.70e-06)	0.007 (2.30e-06)	0.005 (1.60e-06)
Coverage Probabilities			
1e4	0.876 (0.0104)	0.889 (0.0099)	0.596 (0.0155)
1e5	0.880 (0.0103)	0.910 (0.0090)	0.578 (0.0156)
1e6	0.894 (0.0097)	0.913 (0.0094)	0.627 (0.0153)

Thus even simple MCMC problems produce complex dependence structures within and across components of the samples. Ignoring this structure leads to an incomplete

understanding of the estimation process. Not only do we gain more information about the Monte Carlo error using multivariate methods, but we also avoid using conservative Bonferroni methods.

2 Termination Rules

We consider multivariate sequential termination rules that lead to asymptotically valid confidence regions. Let $T_{1-\alpha,p,q}^2$ denote the $1 - \alpha$ quantile of a Hotelling's T-squared distribution with dimensionality parameter p and degrees of freedom q . Throughout this section and the next, we assume Σ_n is a strongly consistent estimator of Σ . A $100(1 - \alpha)\%$ confidence region for θ is the set

$$C_\alpha(n) = \{ \theta \in \mathbb{R}^p : n(\theta_n - \theta)^T \Sigma_n^{-1} (\theta_n - \theta) < T_{1-\alpha,p,q}^2 \},$$

where q is determined by the choice of Σ_n . Then $C_\alpha(n)$ forms an ellipsoid in p dimensions oriented along the directions of the eigenvectors of Σ_n . The volume of $C_\alpha(n)$ is

$$\text{Vol}(C_\alpha(n)) = \frac{2\pi^{p/2}}{p\Gamma(p/2)} \left(\frac{T_{1-\alpha,p,q}^2}{n} \right)^{p/2} |\Sigma_n|^{1/2}. \quad (5)$$

Since p is fixed and $\Sigma_n \rightarrow \Sigma$ with probability 1, $\text{Vol}(C_\alpha(n)) \rightarrow 0$, with probability 1, as $n \rightarrow \infty$. If $\epsilon > 0$ and $s(n)$ is a positive real valued function defined on the positive integers, then a fixed-volume sequential stopping rule terminates the simulation at the random time

$$T(\epsilon) = \inf \left\{ n \geq 0 : \text{Vol}(C_\alpha(n))^{1/p} + s(n) \leq \epsilon \right\}. \quad (6)$$

Glynn and Whitt (1992) provide conditions so that terminating at $T(\epsilon)$ yields confidence regions that are asymptotically valid in that, as $\epsilon \rightarrow 0$, $\Pr[\theta \in C_\alpha(T(\epsilon))] \rightarrow 1 - \alpha$. In particular, they let $s(n) = \epsilon I(n < n^*) + n^{-1}$ which ensures simulation does not terminate

before $n^* \geq 0$ iterations. The sequential stopping rule (6) can be difficult to implement in practice since the choice of ϵ depends on the units of θ , and has to be carefully chosen for every application. We present an alternative to (6) which can be used more naturally and which we will show connects nicely to the idea of ESS.

Let $\|\cdot\|$ denote the Euclidean norm. Let $K(Y, p) > 0$ be an attribute of the estimation process and suppose $K_n(Y, p) > 0$ is an estimator of $K(Y, p)$; for example, take $\|\theta\| = K(Y, p)$ and $\|\theta_n\| = K_n(Y, p)$. Set $s(n) = \epsilon K_n(Y, p) I(n < n^*) + n^{-1}$ and define

$$T^*(\epsilon) = \inf \left\{ n \geq 0 : \text{Vol}(C_\alpha(n))^{1/p} + s(n) \leq \epsilon K_n(Y, p) \right\}.$$

We call $K(Y, p)$ the relative metric. The following result establishes asymptotic validity of this termination rule. The proof is provided in the supplementary material.

Theorem 1. *Let $g : \mathcal{X} \rightarrow \mathbb{R}^p$ be such that $E_F \|g\|^{2+\delta} < \infty$ for some $\delta > 0$ and let X be an F -invariant polynomially ergodic Markov chain of order $m > (1 + \epsilon_1)(1 + 2/\delta)$ for some $\epsilon_1 > 0$. If $K_n(Y, p) \rightarrow K(Y, p)$ with probability 1 and $\Sigma_n \rightarrow \Sigma$ with probability 1, as $n \rightarrow \infty$, then, as $\epsilon \rightarrow 0$, $T^*(\epsilon) \rightarrow \infty$ and $\Pr[\theta \in C_\alpha(T^*(\epsilon))] \rightarrow 1 - \alpha$.*

Remark 1. Theorem 1 applies when $K(Y, p) = K_n(Y, p) = 1$. This choice of the relative metric leads to the absolute-precision fixed-volume sequential stopping rule; a multivariate generalization of the procedure considered by Jones et al. (2006).

Suppose $K(Y, p) = |\Lambda|^{1/2p} = |\text{Var}_F Y_1|^{1/2p}$ and if Λ_n is the usual sample covariance matrix for $\{Y_t\}$, set $K_n(Y, p) = |\Lambda_n|^{1/2p}$. Note that Λ_n is positive definite as long as $n > p$, so $|\Lambda_n|^{1/2p} > 0$. Then $K_n(Y, p) \rightarrow K(Y, p)$, with probability 1, as $n \rightarrow \infty$ and $T^*(\epsilon)$ is the first time the variability in estimation (measured via the volume of the confidence region) is an ϵ th fraction of the variability in the target distribution. The *relative standard deviation fixed-volume sequential stopping rule* is formalized as

terminating at random time

$$T_{SD}(\epsilon) = \inf \left\{ n \geq 0 : \text{Vol}(C_\alpha(n))^{1/p} + \epsilon |\Lambda_n|^{1/2p} I(n < n^*) + n^{-1} \leq \epsilon |\Lambda_n|^{1/2p} \right\}. \quad (7)$$

3 Effective Sample Size

Gong and Flegal (2016), Kass et al. (1998), Liu (2008), and Robert and Casella (2013) define ESS for the i th component of the process as

$$\text{ESS}_i = \frac{n}{1 + 2 \sum_{k=1}^{\infty} \rho(Y_1^{(i)}, Y_{1+k}^{(i)})} = n \frac{\lambda_i^2}{\sigma_i^2},$$

where $\rho(Y_1^{(i)}, Y_{1+k}^{(i)})$ is the lag k correlation for the i th component of Y , σ_i^2 is the i th diagonal element of Σ , and λ_i^2 is the i th diagonal element of Λ . A strongly consistent estimator of ESS_i is obtained through strongly consistent estimators of λ_i^2 and σ_i^2 via the sample variance ($\lambda_{n,i}^2$) and univariate batch means estimators ($\sigma_{n,i}^2$), respectively. ESS_i is then estimated for each component separately, and a conservative estimate of the overall ESS is taken to be the minimum of all ESS_i . This leads to the situation where the estimate of ESS is dictated by the components that mix the slowest, while ignoring all other components.

Instead of using the diagonals of Λ and Σ to define ESS, we use the matrices themselves. Let S_p^+ denote the set of all $p \times p$ positive definite matrices. Univariate quantification of the matrices requires a mapping $S_p^+ \rightarrow \mathbb{R}_+$ that captures the variability described by the covariance matrix. We use the determinant since for a random vector, the determinant of its covariance matrix is its generalized variance. The concept of generalized variance was first introduced by Wilks (1932) as a univariate measure of spread for a multivariate distribution. Wilks (1932) recommended the use of the p th root of the generalized variance. This was formalized by SenGupta (1987) as the *standardized*

generalized variance in order to compare variability over different dimensions. We define

$$\text{ESS} = n \left(\frac{|\Lambda|}{|\Sigma|} \right)^{1/p}.$$

When $p = 1$, the ESS reduces to the form of univariate ESS presented above. Let Λ_n be the sample covariance matrix of $\{Y_t\}$ and Σ_n be a strongly consistent estimator of Σ . Then a strongly consistent estimator of ESS is

$$\widehat{\text{ESS}} = n \left(\frac{|\Lambda_n|}{|\Sigma_n|} \right)^{1/p}.$$

3.1 Lower Bound for Effective Sample Size

Rearranging the defining inequality in (7) yields that when $n \geq n^*$

$$\widehat{\text{ESS}} \geq \left[\left(\frac{2\pi^{p/2}}{p\Gamma(p/2)} \right)^{1/p} (T_{1-\alpha,p,q}^2)^{1/2} + \frac{|\Sigma_n|^{-1/2p}}{n^{1/2}} \right]^2 \frac{1}{\epsilon^2} \approx \frac{2^{2/p}\pi}{(p\Gamma(p/2))^{2/p}} (T_{1-\alpha,p,q}^2) \frac{1}{\epsilon^2}.$$

Thus, the relative standard deviation fixed-volume sequential stopping rule is equivalent to terminating the first time $\widehat{\text{ESS}}$ is larger than a lower bound. This lower bound is a function of n through q and thus is difficult to determine before starting the simulation. However, as $n \rightarrow \infty$, the scaled $T_{p,q}^2$ distribution converges to a χ_p^2 , leading to the following approximation

$$\widehat{\text{ESS}} \geq \frac{2^{2/p}\pi}{(p\Gamma(p/2))^{2/p}} \frac{\chi_{1-\alpha,p}^2}{\epsilon^2}. \quad (8)$$

One can *a priori* determine the number of effective samples required for their choice of ϵ and α . As $p \rightarrow \infty$, the lower bound in (8) converges to $2\pi e/\epsilon^2$. Thus for large p , the lower bound is mainly determined by the choice of ϵ . On the other hand, for a fixed α , having obtained W effective samples, the user can use the lower bound to determine the relative precision (ϵ) in their estimation. In this way, (8) can be used to make informed decisions regarding termination.

Example 1. Suppose $p = 5$ (as in the logistic regression setting of Section 1.1) and that we want a precision of $\epsilon = .05$ (so the Monte Carlo error is 5% of the variability in the target distribution) for a 95% confidence region. This requires $\widehat{\text{ESS}} \geq 8605$. On the other hand, if we simulate until $\widehat{\text{ESS}} = 10000$, we obtain a precision of $\epsilon = .0464$.

Remark 2. Let n_{pos} be the smallest integer such that $\Sigma_{n_{\text{pos}}}$ is positive definite; in the next section we will discuss how to choose n_{pos} for the mBM estimator. In light of the lower bound in (8), a natural choice of n^* is

$$n^* \geq \max \left\{ n_{\text{pos}}, \frac{2^{2/p} \pi}{(p\Gamma(p/2))^{2/p}} \frac{\chi_{1-\alpha, p}^2}{\epsilon^2} \right\}. \quad (9)$$

4 Strong Consistency of Multivariate Batch Means Estimator

In Sections 2 and 3 we assumed the existence of a strongly consistent estimator of Σ . A class of multivariate spectral variance estimators were shown to be strongly consistent by Vats et al. (2017). However, when p is large, this class of estimators is expensive to calculate as we show in Section 6. Thus, we present the relatively inexpensive mBM estimator and provide conditions for strong consistency.

Let $n = a_n b_n$, where a_n is the number of batches and b_n is the batch size. For $k = 0, \dots, a_n - 1$, define $\bar{Y}_k := b_n^{-1} \sum_{t=1}^{b_n} Y_{kb_n+t}$. Then \bar{Y}_k is the mean vector for batch k and the mBM estimator of Σ is given by

$$\Sigma_n = \frac{b_n}{a_n - 1} \sum_{k=0}^{a_n-1} (\bar{Y}_k - \theta_n) (\bar{Y}_k - \theta_n)^T. \quad (10)$$

For the mBM estimator, q in (5) is $a_n - p$. In addition, Σ_n is singular if $a_n < p$, thus n_{pos} is the smallest n such that $a_n > p$.

When Y_t is univariate, the batch means estimator has been well studied for MCMC

problems (Jones et al., 2006; Flegal and Jones, 2010) and for steady state simulations (Damerджи, 1994; Glynn and Iglehart, 1990; Glynn and Whitt, 1991). Glynn and Whitt (1991) showed that the batch means estimator cannot be consistent for fixed batch size, b_n . Damerджи (1994, 1995), Jones et al. (2006) and Flegal and Jones (2010) established its asymptotic properties including strong consistency and mean square consistency when *both* the batch size and number of batches increases with n .

The multivariate extension as in (10) was first introduced by Chen and Seila (1987). For steady-state simulation, Charnes (1995) and Muñoz and Glynn (2001) studied confidence regions for θ based on the mBM estimator, however, its asymptotic properties remain unexplored. In Theorem 2, we present conditions for strong consistency of Σ_n in estimating Σ for MCMC, but our results hold for more general processes. Our main assumption on the process is that of a *strong invariance principle* (SIP).

Condition 1. Let $\|\cdot\|$ denote the Euclidean norm and $\{B(t), t \geq 0\}$ be a p -dimensional multivariate Brownian motion. There exists a $p \times p$ lower triangular matrix L , a non-negative increasing function γ on the positive integers, a finite random variable D , and a sufficiently rich probability space such that, with probability 1, as $n \rightarrow \infty$,

$$\|n(\theta_n - \theta) - LB(n)\| < D\gamma(n). \quad (11)$$

Condition 2. The batch size b_n satisfies the following conditions,

1. the batch size b_n is an integer sequence such that $b_n \rightarrow \infty$ and $n/b_n \rightarrow \infty$ as $n \rightarrow \infty$ where, b_n and n/b_n are monotonically increasing,
2. there exists a constant $c \geq 1$ such that $\sum_n (b_n n^{-1})^c < \infty$.

In Theorem 2 we show strong consistency of Σ_n . The proof is given in the supplementary material

Theorem 2. *Let g be such that $E_F \|g\|^{2+\delta} < \infty$ for some $\delta > 0$. Let X be an F -invariant polynomially ergodic Markov chain of order $m > (1 + \epsilon_1)(1 + 2/\delta)$ for some $\epsilon_1 > 0$. Then (11) holds with $\gamma(n) = n^{1/2-\lambda}$ for some $\lambda > 0$. If Condition 2 holds and $b_n^{-1/2}(\log n)^{1/2}n^{1/2-\lambda} \rightarrow 0$ as $n \rightarrow \infty$, then $\Sigma_n \rightarrow \Sigma$, with probability 1, as $n \rightarrow \infty$.*

Remark 3. The theorem holds more generally outside the context of Markov chains for processes that satisfy Condition 1. This includes independent processes (Berkes and Philipp, 1979; Einmahl, 1989; Zaitsev, 1998), Martingale sequences (Eberlein, 1986), renewal processes (Horvath, 1984) and ϕ -mixing and strongly mixing processes (Kuelbs and Philipp, 1980; Dehling and Philipp, 1982). The general statement of the theorem is provided in the supplementary material

Remark 4. Using Theorem 4 from Kuelbs and Philipp (1980), Vats et al. (2017) established Condition 1 with $\gamma(n) = n^{1/2-\lambda}$, for some $\lambda > 0$ for polynomially ergodic Markov chains. We use their result directly. Kuelbs and Philipp (1980) show that λ only depends on p , ϵ and δ , however the exact relationship remains an open problem. For slow mixing processes λ is closer to 0 while for fast mixing processes λ is closer to 1/2 (Damerджи, 1991, 1994).

Remark 5. It is natural to consider $b_n = \lfloor n^\nu \rfloor$ for $0 < \nu < 1$. Then λ in the SIP must satisfy $\lambda > (1 - \nu)/4$ so that $b_n^{-1/2}(\log n)^{1/2}n^{1/2-\lambda} \rightarrow 0$ as $n \rightarrow \infty$. Since $\nu > 1 - 2\lambda$, smaller batch sizes suffice for fast mixing processes and slow mixing processes require larger batch sizes. This reinforces our intuition that higher correlation calls for larger batch sizes. Calibrating ν in $b_n = \lfloor n^\nu \rfloor$ is essential to ensuring the mBM estimates perform well in finite samples. Using mean square consistency of univariate batch means estimators, Flegal and Jones (2010) concluded that an asymptotically optimal batch size is proportional to $\lfloor n^{1/3} \rfloor$.

Remark 6. For $p = 1$, Jones et al. (2006) proved strong consistency of the batch means estimator under the stronger assumption of geometric ergodicity and a one-step mi-

norization, which we do not make. Thus, in Theorem 2 while extending the result of strong consistency to $p \geq 1$, we also weaken the conditions for the univariate case.

Remark 7. By Theorem 3 in Vats et al. (2017), strong consistency of the mBM estimator implies strong consistency of its eigenvalues.

5 Examples

In each of the following examples we present a target distribution F , a Markov chain with F as its invariant distribution, we specify g , and are interested in estimating $E_F g$. We consider the finite sample performance (based on 1000 independent replications) of the relative standard deviation fixed-volume sequential stopping rules and compare them to the relative standard deviation fixed-width sequential stopping rules (see Flegal and Gong (2015) and the supplementary material). In each case we make 90% confidence regions for various choices of ϵ and specify our choice of n^* and b_n . The sequential stopping rules are checked at 10% increments of the current Monte Carlo sample size.

5.1 Bayesian Logistic Regression

We continue the Bayesian logistic regression example of Section 1.1. Recall that a random walk Metropolis-Hastings algorithm was implemented to sample from the intractable posterior. We prove the chain is geometrically ergodic in the supplementary material.

Theorem 3. *The random walk based Metropolis-Hastings algorithm with invariant distribution given by the posterior from (4) is geometrically ergodic.*

As a consequence of Theorem 3 and that F has a moment generating function, the conditions of Theorems 1 and 2 hold.

Motivated by the ACF plot in Figure 1a, b_n was set to $\lfloor n^{1/2} \rfloor$ and $n^* = 1000$. For calculating coverage probabilities, we declare the “truth” as the posterior mean from an independent simulation of length 10^9 . The results are presented in Table 2. As before,

the univariate uncorrected method has poor coverage probabilities. For $\epsilon = 0.02$ and 0.01 , the coverage probabilities for both the mBM and uBM-Bonferroni regions are at 90%. However, termination for mBM is significantly earlier.

Table 2: Bayesian Logistic Regression: Over 1000 replications, we present termination iterations, effective sample size at termination and coverage probabilities at termination for each corresponding method. Standard errors are in parenthesis.

	mBM	uBM-Bonferroni	uBM
Termination Iteration			
$\epsilon = 0.05$	133005 (196)	201497 (391)	100445 (213)
$\epsilon = 0.02$	844082 (1158)	1262194 (1880)	629898 (1036)
$\epsilon = 0.01$	3309526 (1837)	5046449 (7626)	2510673 (3150)
Effective Sample Size			
$\epsilon = 0.05$	7712 (9)	9270 (13)	4643 (7)
$\epsilon = 0.02$	47862 (51)	57341 (65)	28768 (36)
$\epsilon = 0.01$	186103 (110)	228448 (271)	113831 (116)
Coverage Probabilities			
$\epsilon = 0.05$	0.889 (0.0099)	0.909 (0.0091)	0.569 (0.0157)
$\epsilon = 0.02$	0.896 (0.0097)	0.912 (0.0090)	0.606 (0.0155)
$\epsilon = 0.01$	0.892 (0.0098)	0.895 (0.0097)	0.606 (0.0155)

Recall from Theorem 1, as ϵ decreases to zero, the coverage probability of confidence regions created at termination using the relative standard deviation fixed-volume sequential stopping rule converges to the nominal level. This is demonstrated in Figure 2 where we present the coverage probability over 1000 replications as $-\epsilon$ increases (or ϵ decreases). Notice that the increase in coverage probabilities need not be monotonic due to the underlying randomness.

5.2 Vector Autoregressive Process

Consider the vector autoregressive process of order 1 (VAR(1)). For $t = 1, 2, \dots$,

$$Y_t = \Phi Y_{t-1} + \epsilon_t,$$

where $Y_t \in \mathbb{R}^p$, Φ is a $p \times p$ matrix, $\epsilon_t \stackrel{iid}{\sim} N_p(0, \Omega)$, and Ω is a $p \times p$ positive definite matrix. The matrix Φ determines the nature of the autocorrelation. This Markov chain

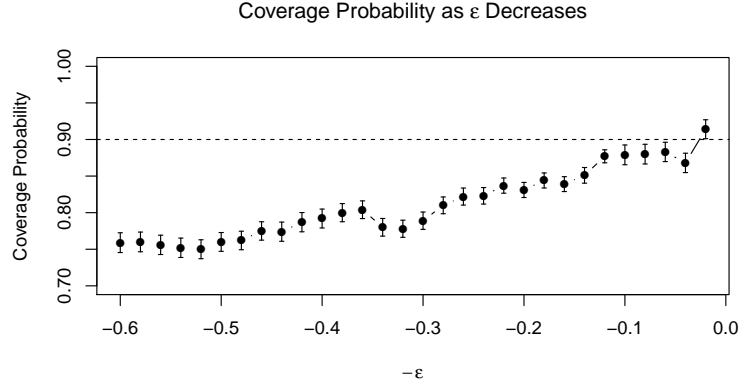


Figure 2: Bayesian Logistic: Plot of coverage probability with confidence bands as ε decreases at 90% nominal rate. Replications = 1000.

has invariant distribution $F = N_p(0, V)$ where $vec(V) = (I_{p^2} - \Phi \otimes \Phi)^{-1}vec(\Omega)$, \otimes denotes the Kronecker product, and is geometrically ergodic when the spectral radius of Φ is less than 1 (Tjøstheim, 1990).

Consider the goal of estimating the mean of F , $E_F Y = 0$ with \bar{Y}_n . Then

$$\Sigma = (I_p - \Phi)^{-1}V + V(I_p - \Phi)^{-1} - V.$$

Let $p = 5$, $\Phi = \text{diag}(.9, .5, .1, .1, .1)$, and Ω be the AR(1) covariance matrix with autocorrelation 0.9. Since the first eigenvalue of Φ is large, the first component mixes slowest. We sample the process for 10^5 iterations and in Figure 3a present the ACF plot for $Y^{(1)}$ and $Y^{(3)}$ and the cross-correlation (CCF) plot between $Y^{(1)}$ and $Y^{(3)}$ in addition to the trace plot for $Y^{(1)}$. Notice that $Y^{(1)}$ exhibits higher autocorrelation than $Y^{(3)}$ and there is significant cross-correlation between $Y^{(1)}$ and $Y^{(3)}$.

Figure 3b displays joint confidence regions for $Y^{(1)}$ and $Y^{(3)}$. Recall that the true mean is $(0, 0)$, and is present in all three regions, but the ellipse produced by mBM has significantly smaller volume than the uBM boxes. The orientation of the ellipse is determined by the cross-correlations witnessed in Figure 3a.

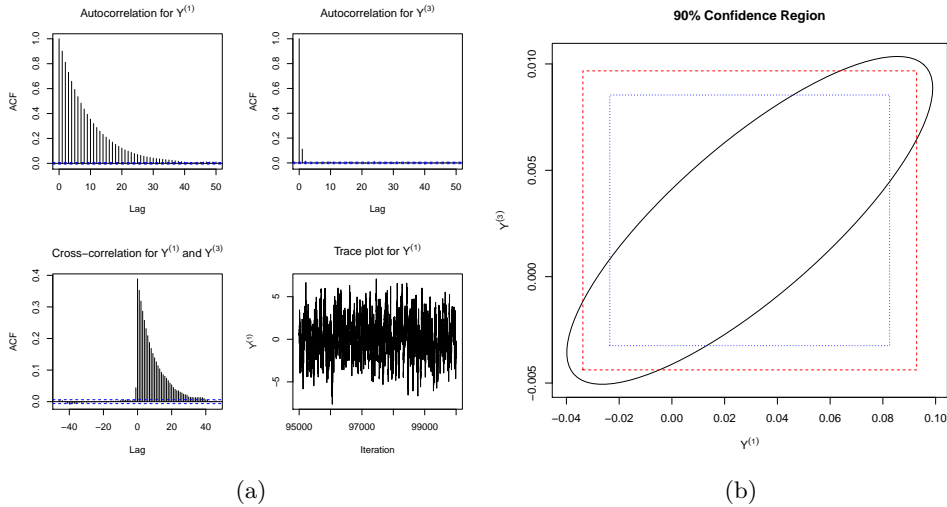


Figure 3: VAR: (a) ACF plot for $Y^{(1)}$ and $Y^{(3)}$, CCF plot between $Y^{(1)}$ and $Y^{(3)}$, and trace plot for $Y^{(1)}$. Monte Carlo sample size is 10^5 . (b) Joint 90% confidence region for first the two components of Y . The solid ellipse is made using mBM, the dotted box using uBM uncorrected and the dashed line using uBM corrected by Bonferroni. The Monte Carlo sample size is 10^5 .

We set $n^* = 1000$, $b_n = \lfloor n^{1/2} \rfloor$, ϵ in $\{0.05, 0.02, 0.01\}$ and at termination of each method, calculate the coverage probabilities and effective sample size. Results are presented in Table 3. Note that as ϵ decreases, termination time increases and coverage probabilities tend to the 90% nominal for each method. Also note that the uncorrected methods produce confidence regions with undesirable coverage probabilities and thus are not of interest. Consider $\epsilon = .02$ in Table 3. Termination for mBM is at $8.8e4$ iterations compared to $9.6e5$ for uBM-Bonferroni. However, the estimates for multivariate ESS at $8.8e4$ iterations is $4.7e4$ samples compared to univariate ESS of $5.6e4$ samples for $9.6e5$ iterations. This is because the leading component $Y^{(1)}$ mixes much slower than the other components and defines the behavior of the univariate ESS.

A small study presented in Table 4 elaborates on this behavior. We present the mean estimate of ESS using multivariate and univariate methods based on 100 replications of Monte Carlo sample sizes 10^5 and 10^6 . The estimate of ESS for the first component is significantly smaller than all other components leading to a conservative univariate

Table 3: VAR: Over 1000 replications, we present termination iterations, effective sample size at termination and coverage probabilities at termination for each corresponding method. Standard errors are in parentheses.

	mBM	uBM-Bonferroni	uBM
Termination Iteration			
$\epsilon = 0.05$	14574 (27)	169890 (393)	83910 (222)
$\epsilon = 0.02$	87682 (118)	1071449 (1733)	533377 (1015)
$\epsilon = 0.01$	343775 (469)	4317599 (5358)	2149042 (3412)
Effective Sample Size			
$\epsilon = 0.05$	8170 (11)	9298 (13)	4658 (7)
$\epsilon = 0.02$	48659 (50)	57392 (68)	28756 (37)
$\epsilon = 0.01$	190198 (208)	228772 (223)	114553 (137)
Coverage Probabilities			
$\epsilon = 0.05$	0.911 (0.0090)	0.940 (0.0075)	0.770 (0.0133)
$\epsilon = 0.02$	0.894 (0.0097)	0.950 (0.0069)	0.769 (0.0133)
$\epsilon = 0.01$	0.909 (0.0091)	0.945 (0.0072)	0.779 (0.0131)

estimate of ESS.

Table 4: VAR: Effective sample size (ESS) estimated using proposed multivariate method and the univariate method of Gong and Flegal (2016) for Monte Carlo sample sizes of $n = 1e5, 1e6$ and 100 replications. Standard errors are in parentheses.

n	ESS	ESS ₁	ESS ₂	ESS ₃	ESS ₄	ESS ₅
1e5	55190 (200)	5432 (41)	33707 (280)	82485 (728)	82903 (731)	82370 (726)
1e6	551015 (945)	53404 (193)	334656 (1345)	819449 (3334)	819382 (3209)	819840 (2858)

5.3 Bayesian Lasso

Let y be a $K \times 1$ response vector and X be a $K \times r$ matrix of predictors. We consider the following Bayesian lasso formulation of Park and Casella (2008).

$$\begin{aligned}
 y|\beta, \sigma^2, \tau^2 &\sim N_K(X\beta, \sigma^2 I_n) \\
 \beta|\sigma^2, \tau^2 &\sim N_r(0, \sigma^2 D_\tau) \quad \text{where} \quad D_\tau = \text{diag}(\tau_1^2, \tau_2^2, \dots, \tau_r^2) \\
 \sigma^2 &\sim \text{Inverse-Gamma}(\alpha, \xi) \\
 \tau_j^2 &\stackrel{iid}{\sim} \text{Exponential}\left(\frac{\lambda^2}{2}\right) \quad \text{for } j = 1, \dots, r,
 \end{aligned}$$

where λ, α , and ξ are fixed and the Inverse-Gamma(a, b) distribution with density proportional to $x^{-a-1}e^{-b/x}$. We use a deterministic scan Gibbs sampler to draw approximate samples from the posterior; see Khare and Hobert (2013) for a full description of the algorithm. Khare and Hobert (2013) showed that for $K \geq 3$, this Gibbs sampler is geometrically ergodic for arbitrary r, X , and λ .

We fit this model to the cookie dough dataset of Osborne et al. (1984). The data was collected to test the feasibility of near infra-red (NIR) spectroscopy for measuring the composition of biscuit dough pieces. There are 72 observations. The response variable is the amount of dry flour content measured and the predictor variables are 25 measurements of spectral data spaced equally between 1100 to 2498 nanometers. Since we are interested in estimating the posterior mean for $(\beta, \tau^2, \sigma^2)$, $p = 51$. The data is available in the R package `ppls`, and the Gibbs sampler is implemented in function `blasso` in R package `monomvn`. The “truth” was declared by averaging posterior means from 1000 independent runs each of length 1e6. We set $n^* = 2e4$ and $b_n = \lfloor n^{1/3} \rfloor$.

In Table 5 we present termination results from 1000 replications. With $p = 51$, the uncorrected univariate regions produce confidence regions with low coverage probabilities. The uBM-Bonferroni and mBM provide competitive coverage probabilities at termination. However, termination for mBM is significantly earlier than univariate methods over all values of ϵ . For $\epsilon = .05$ and $.02$ we observe zero standard error for termination using mBM since termination is achieved at the same 10% increment over all 1000 replications. Thus the variability in those estimates is less than 10% of the size of the estimate.

5.4 Bayesian Dynamic Spatial-Temporal Model

Gelfand et al. (2005) propose a Bayesian hierarchical model for modeling univariate and multivariate dynamic spatial data viewing time as discrete and space as continuous. The methods in their paper have been implemented in the R package `spBayes`. We present

Table 5: Bayesian Lasso: Over 1000 replications, we present termination iterations, effective sample size at termination and coverage probabilities at termination for each corresponding method. Standard errors are in parentheses.

	mBM	uBM-Bonferroni	uBM
Termination Iteration			
$\epsilon = 0.05$	20000 (0)	69264 (76)	20026 (7)
$\epsilon = 0.02$	69045 (0)	445754 (664)	122932 (103)
$\epsilon = 0.01$	271088 (393)	1765008 (431)	508445 (332)
Effective Sample Size			
$\epsilon = 0.05$	15631 (4)	16143 (15)	4778 (6)
$\epsilon = 0.02$	52739 (8)	101205 (122)	28358 (24)
$\epsilon = 0.01$	204801 (283)	395480 (163)	115108 (74)
Coverage Probabilities			
$\epsilon = 0.05$	0.898 (0.0096)	0.896 (0.0097)	0.010 (0.0031)
$\epsilon = 0.02$	0.892 (0.0098)	0.905 (0.0093)	0.009 (0.0030)
$\epsilon = 0.01$	0.898 (0.0096)	0.929 (0.0081)	0.009 (0.0030)

a simpler version of the dynamic model as described by Finley et al. (2015).

Let $s = 1, 2, \dots, N_s$ be location sites, $t = 1, 2, \dots, N_t$ be time-points, and the observed measurement at location s and time t be denoted by $y_t(s)$. In addition, let $x_t(s)$ be the $r \times 1$ vector of predictors, observed at location s and time t , and β_t be the $r \times 1$ vector of coefficients. For $t = 1, 2, \dots, N_t$,

$$y_t(s) = x_t(s)^T \beta_t + u_t(s) + \epsilon_t(s), \quad \epsilon_t(s) \stackrel{ind}{\sim} N(0, \tau_t^2); \quad (12)$$

$$\beta_t = \beta_{t-1} + \eta_t, \quad \eta_t \stackrel{iid}{\sim} N(0, \Sigma_\eta);$$

$$u_t(s) = u_{t-1}(s) + w_t(s), \quad w_t(s) \stackrel{ind}{\sim} GP(0, \sigma_t^2 \rho(\cdot; \phi_t)), \quad (13)$$

where $GP(0, \sigma_t^2 \rho(\cdot; \phi_t))$ denotes a spatial Gaussian process with covariance function $\sigma_t^2 \rho(\cdot; \phi_t)$. Here, σ_t^2 denotes the spatial variance component and $\rho(\cdot, \phi_t)$ is the correlation function with exponential decay. Equation (12) is referred to as the measurement equation and $\epsilon_t(s)$ denotes the measurement error, assumed to be independent of location and time. Equation (13) contains the transition equations which emulate the Markovian nature of dependence in time. To complete the Bayesian hierarchy, the following priors

are assumed

$$\begin{aligned}\beta_0 &\sim N(m_0, C_0) & \text{and} & & u_0(s) &\equiv 0; \\ \tau_t^2 &\sim \text{IG}(a_\tau, b_\tau) & \text{and} & & \sigma_t^2 &\sim \text{IG}(a_s, b_s); \\ \Sigma_\eta &\sim \text{IW}(a_\eta, B_\eta) & \text{and} & & \phi_t &\sim \text{Unif}(a_\phi, b_\phi),\end{aligned}$$

where IW is the Inverse-Wishart distribution with probability density function proportional to $|\Sigma_\eta|^{-\frac{a_\eta+q+1}{2}} e^{-\frac{1}{2}\text{tr}(B_\eta\Sigma_\eta^{-1})}$ and $\text{IG}(a, b)$ is the Inverse-Gamma distribution with density proportional to $x^{-a-1}e^{-b/x}$. We fit the model to the **NETemp** dataset in the **spBayes** package. This dataset contains monthly temperature measurements from 356 weather stations on the east coast of the USA collected from January 2000 to December 2010. The elevation of the weather stations is also available as a covariate. We choose a subset of the data with 10 weather stations for the year 2000, and fit the model with an intercept. The resulting posterior has $p = 185$ components.

A component-wise Metropolis-Hastings sampler (Johnson et al., 2013; Jones et al., 2014) is described in Gelfand et al. (2005) and implemented in the **spDynLM** function. Default hyper parameter settings were used. The posterior and the rate of convergence for this sampler have not been studied; thus we do not know if the conditions of our theoretical results are satisfied. Our goal is to estimate the posterior expectation of $\theta = (\beta_t, u_t(s), \sigma_t^2, \Sigma_\eta, \tau_t^2, \phi_t)$. The truth was declared by averaging over 1000 independent runs of length $2e6$ MCMC samples. We set $b_n = \lfloor n^{1/2} \rfloor$ and $n^* = 5e4$ so that $a_n > p$ to ensure positive definitiveness of Σ_n .

Due to the Markovian transition equations in (13), the β_t and u_t exhibit a significant covariance in the posterior distribution. This is evidenced in Figure 4 where for Monte Carlo sample size $n = 10^5$, we present confidence regions for $\beta_1^{(0)}$ and $\beta_2^{(0)}$ which are the intercept coefficient for the first and second months, and for $u_1(1)$ and $u_2(1)$ which are the additive spatial coefficients for the first two weather stations. The thin ellipses

indicate that the principle direction of variation is due to the correlation between the components. This significant reduction in volume, along with the conservative Bonferroni correction ($p = 185$) results in increased delay in termination when using univariate methods. For smaller values of ϵ it was not possible to store the MCMC output in memory on a 8 gigabyte machine using uBM-Bonferroni methods. As a result (see Table 6),

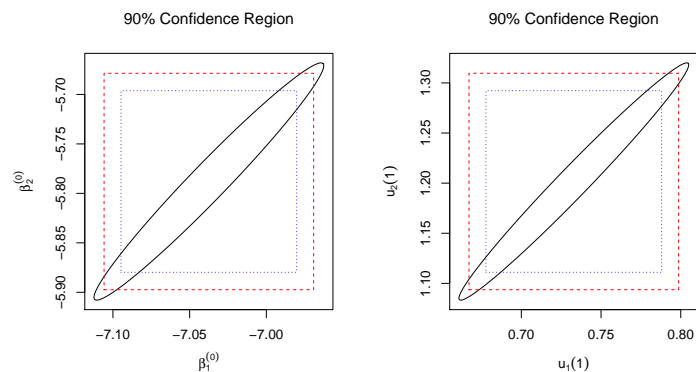


Figure 4: Bayesian Spatial: 90% confidence regions for $\beta_1^{(0)}$ and $\beta_2^{(0)}$ and $u_1(1)$ and $u_2(1)$. The Monte Carlo sample size = 10^5 .

the univariate methods could not be implemented for smaller ϵ values. For $\epsilon = .10$, termination for mBM was at $n^* = 5e4$ for every replication. At these minimum iterations, the coverage probability for mBM is at 88%, whereas both the univariate methods have far lower coverage probabilities at 0.62 for uBM-Bonferroni and 0.003 for uBM. The coverage probabilities for the uncorrected methods are quite small since we are making 185 confidence regions simultaneously.

6 Discussion

Multivariate analysis of MCMC output data has received little attention. Seila (1982) and Chen and Seila (1987) built a framework for multivariate analysis for a Markov chain using regenerative simulation. Since establishing regenerative properties for a Markov chain requires a separate analysis for every problem and will not work well in component-

Table 6: Bayesian Spatial: Over 1000 replications, we present termination iteration, effective sample size at termination and coverage probabilities at termination for each corresponding method at 90% nominal levels. Standard errors are in parentheses.

	mBM	uBM-Bonferroni	uBM
Termination Iteration			
$\epsilon = 0.10$	50000 (0)	1200849 (28315)	311856 (491)
$\epsilon = 0.05$	50030 (12)	-	1716689 (2178)
$\epsilon = 0.02$	132748 (174)	-	-
Effective Sample Size			
$\epsilon = 0.10$	55170 (20)	3184 (75)	1130 (1)
$\epsilon = 0.05$	55190 (20)	-	4525 (4)
$\epsilon = 0.02$	105166 (97)	-	-
Coverage Probabilities			
$\epsilon = 0.10$	0.882 (0.0102)	0.625 (0.0153)	0.007 (0.0026)
$\epsilon = 0.05$	0.881 (0.0102)	-	0.016 (0.0040)
$\epsilon = 0.02$	0.864 (0.0108)	-	-

wise Metropolis-Hastings samplers, the application of their work is limited. Paul et al. (2012) used a specific multivariate Markov chain CLT for their MCMC convergence diagnostic. More recently, Vats et al. (2017) showed strong consistency of the multivariate spectral variance (mSV) estimators of Σ , which could potentially substitute for the mBM estimator in applications to termination rules. However, outside of toy problems where p is small, the mSV estimator is computationally demanding compared to the mBM estimator. To compare these two estimators, we extend the VAR(1) example discussed in Section 5.2, to $p = 50$. Since in this case we know the true Σ , we assess the relative error in estimation $\|\hat{\Sigma} - \Sigma\|_F / \|\Sigma\|_F$ where $\hat{\Sigma}$ is either the mBM or mSV estimator and $\|\cdot\|_F$ is the Frobenius norm. The results are reported in Table 7. The mSV estimator overall has slightly smaller relative error, but as the Monte Carlo sample size increases, computation time is significantly higher than the mBM estimator. Also note that the relative error for both estimators decreases with an increase in Monte Carlo sample size. The mSV and mBM estimators along with multivariate ESS have been implemented in the `mcmcse` R package (Flegal et al., 2017).

There are two aspects of the proposed methodology that will benefit from further

Table 7: Relative error and computation time (in seconds) comparison between mSV and mBM estimators for a VAR(1) model with $p = 50$ over varying Monte Carlo samples sizes. Standard errors are in parentheses.

Method	n	Relative Error	Computation Time
mBM	1e3	0.373 (0.00374)	0.00069 (1.5e-05)
mSV	1e3	0.371 (0.00375)	0.06035 (2.1e-05)
mBM	1e4	0.177 (0.00205)	0.00376 (1.7e-05)
mSV	1e4	0.163 (0.00197)	2.13193 (1.8e-04)
mBM	1e5	0.095 (0.00113)	0.04038 (8.6e-05)
mSV	1e5	0.081 (0.00100)	68.2796 (0.11416)

research. First, the rate of convergence of the Markov chain affects the choice of b_n through the λ in the SIP. Aside from Damerджи (1995) and Flegel and Jones (2010), little work has been done in optimal batch size selection for batch means estimators. This area warrants further research both in asymptotic and finite sample optimal batch selection. In the supplement we study the effect of different batch sizes on simulation termination using the relative standard deviation fixed-volume sequential stopping rule. We notice that a decrease in the tolerance level ϵ , decreases the sensitivity of termination to the choice of b_n . We have found that using a large batch size such as $b_n = \lfloor n^{1/2} \rfloor$ often works well.

Second, when using the mBM estimator, a truly large p requires a large Monte Carlo sample size to ensure a positive definite estimate of Σ . The mSV estimator might yield positive definite estimates at smaller sample sizes, but is far too computationally expensive (see Table 7). It could be interesting to investigate the use of dimension reduction techniques or high-dimensional asymptotics to address this problem.

References

- Acosta, F., Huber, M. L., and Jones, G. L. (2015). Markov chain Monte Carlo with lynchpin variables. *Preprint*.
- Atchadé, Y. F. (2011). Kernel estimators of asymptotic variance for adaptive Markov

- chain Monte Carlo. *The Annals of Statistics*, 39:990–1011.
- Atchadé, Y. F. (2016). Markov chain Monte Carlo confidence intervals. *Bernoulli*, 22:1808–1838.
- Atkinson, Q. D., Gray, R. D., and Drummond, A. J. (2008). mtDNA variation predicts population size in humans and reveals a major southern Asian chapter in human prehistory. *Molecular Biology and Evolution*, 25(2):468–474.
- Berkes, I. and Philipp, W. (1979). Approximation theorems for independent and weakly dependent random vectors. *The Annals of Probability*, 7:29–54.
- Billingsley, P. (1968). *Convergence of Probability Measures*. Wiley, New York.
- Charnes, J. M. (1995). Analyzing multivariate output. In *Proceedings of the 27th conference on Winter simulation*, pages 201–208. IEEE Computer Society.
- Chen, D.-F. R. and Seila, A. F. (1987). Multivariate inference in stationary simulation using batch means. In *Proceedings of the 19th conference on Winter simulation*, pages 302–304. ACM.
- Csörgő, M. and Révész, P. (1981). *Strong Approximations in Probability and Statistics*. Academic Press.
- Dai, N. and Jones, G. L. (2017). Multivariate initial sequence estimators in Markov chain Monte Carlo. *Preprint*.
- Damerdji, H. (1991). Strong consistency and other properties of the spectral variance estimator. *Management Science*, 37:1424–1440.
- Damerdji, H. (1994). Strong consistency of the variance estimator in steady-state simulation output analysis. *Mathematics of Operations Research*, 19:494–512.

- Damerджи, H. (1995). Mean-square consistency of the variance estimator in steady-state simulation output analysis. *Operations Research*, 43(2):282–291.
- Dehling, H. and Philipp, W. (1982). Almost sure invariance principles for weakly dependent vector-valued random variables. *The Annals of Probability*, 10:689–701.
- Doss, H. and Hobert, J. P. (2010). Estimation of Bayes factors in a class of hierarchical random effects models using a geometrically ergodic MCMC algorithm. *Journal of Computational and Graphical Statistics*, 19:295–312.
- Drummond, A. J., Ho, S. Y., Phillips, M. J., and Rambaut, A. (2006). Relaxed phylogenetics and dating with confidence. *PLoS Biology*, 4(5):699.
- Eberlein, E. (1986). On strong invariance principles under dependence assumptions. *The Annals of Probability*, 14:260–270.
- Einmahl, U. (1989). Extensions of results of Komlós, Major, and Tusnády to the multivariate case. *Journal of Multivariate Analysis*, 28:20–68.
- Finley, A., Banerjee, S., and Gelfand, A. (2015). spbayes for large univariate and multivariate point-referenced spatio-temporal data models. *Journal of Statistical Software*, 63(13):1–28.
- Flegal, J. M. and Gong, L. (2015). Relative fixed-width stopping rules for Markov chain Monte Carlo simulations. *Statistica Sinica*, 25:655–676.
- Flegal, J. M., Haran, M., and Jones, G. L. (2008). Markov chain Monte Carlo: Can we trust the third significant figure? *Statistical Science*, 23:250–260.
- Flegal, J. M., Hughes, J., Vats, D., and Dai, N. (2017). *mcmcse: Monte Carlo Standard Errors for MCMC*. Riverside, CA and Minneapolis, MN. R package version 1.3-2.
- Flegal, J. M. and Jones, G. L. (2010). Batch means and spectral variance estimators in Markov chain Monte Carlo. *The Annals of Statistics*, 38:1034–1070.

- Gelfand, A. E., Banerjee, S., and Gamerman, D. (2005). Spatial process modelling for univariate and multivariate dynamic spatial data. *Environmetrics*, 16:465–479.
- Gelman, A. and Rubin, D. B. (1992). Inference from iterative simulation using multiple sequences (with discussion). *Statistical Science*, 7:457–472.
- Giordano, R., Broderick, T., and Jordan, M. (2015). Linear response methods for accurate covariance estimates from mean field variational Bayes. In *Advances in Neural Information Processing Systems*, pages 1441–1449.
- Glynn, P. W. and Iglehart, D. L. (1990). Simulation output analysis using standardized time series. *Mathematics of Operations Research*, 15:1–16.
- Glynn, P. W. and Whitt, W. (1991). Estimating the asymptotic variance with batch means. *Operations Research Letters*, 10:431–435.
- Glynn, P. W. and Whitt, W. (1992). The asymptotic validity of sequential stopping rules for stochastic simulations. *The Annals of Applied Probability*, 2:180–198.
- Gong, L. and Flegal, J. M. (2016). A practical sequential stopping rule for high-dimensional Markov chain Monte Carlo. *Journal of Computational and Graphical Statistics*, 25(3):684–700.
- Hobert, J. P. and Geyer, C. J. (1998). Geometric ergodicity of Gibbs and block Gibbs samplers for a hierarchical random effects model. *Journal of Multivariate Analysis*, 67:414–430.
- Horvath, L. (1984). Strong approximation of extended renewal processes. *The Annals of Probability*, 12:1149–1166.
- Jarner, S. F. and Hansen, E. (2000). Geometric ergodicity of Metropolis algorithms. *Stochastic Processes and Their Applications*, 85:341–361.

- Jarner, S. F. and Roberts, G. O. (2002). Polynomial convergence rates of Markov chains. *Annals of Applied Probability*, 12:224–247.
- Johnson, A. A. and Jones, G. L. (2015). Geometric ergodicity of random scan Gibbs samplers for hierarchical one-way random effects models. *Journal of Multivariate Analysis*, 140:325–342.
- Johnson, A. A., Jones, G. L., and Neath, R. C. (2013). Component-wise Markov chain Monte Carlo. *Statistical Science*, 28(3):360–375.
- Jones, G. L. (2004). On the Markov chain central limit theorem. *Probability Surveys*, 1:299–320.
- Jones, G. L., Haran, M., Caffo, B. S., and Neath, R. (2006). Fixed-width output analysis for Markov chain Monte Carlo. *Journal of the American Statistical Association*, 101:1537–1547.
- Jones, G. L. and Hobert, J. P. (2004). Sufficient burn-in for Gibbs samplers for a hierarchical random effects model. *The Annals of Statistics*, 32:784–817.
- Jones, G. L., Roberts, G. O., and Rosenthal, J. S. (2014). Convergence of conditional Metropolis-Hastings samplers. *Advances in Applied Probability*, 46:422–445.
- Kass, R. E., Carlin, B. P., Gelman, A., and Neal, R. M. (1998). Markov chain Monte Carlo in practice: a roundtable discussion. *The American Statistician*, 52(2):93–100.
- Kendall, M. G. and Stuart, A. (1963). *The Advanced Theory of Statistics*, volume 1. Charles Griffen & Company Limited, London, second edition.
- Khare, K. and Hobert, J. P. (2013). Geometric ergodicity of the Bayesian lasso. *Electronic Journal of Statistics*, 7:2150–2163.
- Kruschke, J. (2014). *Doing Bayesian Data Analysis: A Tutorial with R, JAGS, and Stan*. Academic Press.

- Kuelbs, J. and Philipp, W. (1980). Almost sure invariance principles for partial sums of mixing B-valued random variables. *The Annals of Probability*, 8:1003–1036.
- Liu, J. S. (2008). *Monte Carlo Strategies in Scientific Computing*. Springer, New York.
- Marchev, D. and Hobert, J. P. (2004). Geometric ergodicity of van Dyk and Meng’s algorithm for the multivariate Student’s t model. *Journal of the American Statistical Association*, 99:228–238.
- Muñoz, D. F. and Glynn, P. W. (2001). Multivariate standardized time series for steady-state simulation output analysis. *Operations Research*, 49:413–422.
- Osborne, B. G., Fearn, T., Miller, A. R., and Douglas, S. (1984). Application of near infrared reflectance spectroscopy to the compositional analysis of biscuits and biscuit doughs. *Journal of the Science of Food and Agriculture*, 35:99–105.
- Park, T. and Casella, G. (2008). The Bayesian lasso. *Journal of the American Statistical Association*, 103(482):681–686.
- Paul, R., MacEachern, S. N., and Berliner, L. M. (2012). Assessing convergence and mixing of MCMC implementations via stratification. *Journal of Computational and Graphical Statistics*, 21:693–712.
- Robert, C. P. and Casella, G. (2013). *Monte Carlo Statistical Methods*. Springer, New York.
- Roberts, G. O., Gelman, A., and Gilks, W. R. (1997). Weak convergence and optimal scaling of random walk Metropolis algorithms. *The Annals of Applied Probability*, 7:110–120.
- Roberts, G. O. and Polson, N. G. (1994). On the geometric convergence of the Gibbs sampler. *Journal of the Royal Statistical Society, Series B*, 56:377–384.

- Seila, A. F. (1982). Multivariate estimation in regenerative simulation. *Operations Research Letters*, 1:153–156.
- SenGupta, A. (1987). Tests for standardized generalized variances of multivariate normal populations of possibly different dimensions. *Journal of Multivariate Analysis*, 23:209–219.
- Tan, A. and Hobert, J. P. (2012). Block Gibbs sampling for Bayesian random effects models with improper priors: Convergence and regeneration. *Journal of Computational and Graphical Statistics*, 18:861–878.
- Tan, A., Jones, G. L., and Hobert, J. P. (2013). On the geometric ergodicity of two-variable Gibbs samplers. In Jones, G. L. and Shen, X., editors, *Advances in Modern Statistical Theory and Applications: A Festschrift in honor of Morris L. Eaton*, pages 25–42. Institute of Mathematical Statistics, Beachwood, Ohio.
- Tjøstheim, D. (1990). Non-linear time series and Markov chains. *Advances in Applied Probability*, 22:587–611.
- Vats, D. (2016). Geometric ergodicity of Gibbs samplers in Bayesian penalized regression models. *arXiv preprint arXiv:1609.04057*.
- Vats, D., Flegal, J. M., and Jones, G. L. (2017). Strong consistency of multivariate spectral variance estimators in Markov chain Monte Carlo. *Bernoulli*, (to appear).
- Wilks, S. S. (1932). Certain generalizations in the analysis of variance. *Biometrika*, pages 471–494.
- Zaitsev, A. Y. (1998). Multidimensional version of the results of Komlós and Tusnády for vectors with finite exponential moments. *ESAIM: Probability and Statistics*, 2:41–108.

SUPPLEMENTARY MATERIAL

A Appendix

B Proof of Theorem 1

By Vats et al. (2017), since $E_F \|g\|^{2+\delta} < \infty$ and $\{X_t\}$ is polynomially ergodic of order $k > (1 + \epsilon_1)(1 + 2/\delta)$, Condition 1 holds with $\gamma(n) = n^{1/2-\lambda}$ for $\lambda > 0$. This implies the existence of an FCLT. Now, recall that

$$T^*(\epsilon) = \inf \left\{ n \geq 0 : \text{Vol}(C_\alpha(n))^{1/p} + s(n) \leq \epsilon K_n(Y, p) \right\}.$$

For cleaner notation we will use K_n for $K_n(Y, p)$ and K for $K(Y, p)$. First, we show that as $\epsilon \rightarrow 0$, $T^*(\epsilon) \rightarrow \infty$. Recall $s(n) = \epsilon K_n I(n < n^*) + n^{-1}$. Consider the rule,

$$t(\epsilon) = \inf \{ n \geq 0 : s(n) < \epsilon K_n \} = \inf \{ n \geq 0 : \epsilon I(n < n^*) + (K_n n)^{-1} < \epsilon \}.$$

As $\epsilon \rightarrow 0$, $t(\epsilon) \rightarrow \infty$. Since $T^*(\epsilon) > t(\epsilon)$, $T^*(\epsilon) \rightarrow \infty$ as $\epsilon \rightarrow 0$.

Define $V(n) = \text{Vol}(C_\alpha(n))^{1/p} + s(n)$. Then

$$T^*(\epsilon) = \inf \{ n \geq 0 : V(n) \leq \epsilon K_n \}.$$

Let

$$d_{\alpha,p} = \frac{2\pi^{p/2}}{p\Gamma(p/2)} (\chi_{1-\alpha,p}^2)^{p/2}.$$

Since $s(n) = o(n^{-1/2})$ and Σ is positive definite,

$$\begin{aligned} n^{1/2}V(n) &= n^{1/2} \left[n^{-1/2} \left(\frac{2\pi^{p/2}}{p\Gamma(p/2)} \left(\frac{p(a_n-1)}{(a_n-p)} F_{1-\alpha,p,a_n-p} \right)^{p/2} |\Sigma_n|^{1/2} \right)^{1/p} + s(n) \right] \\ &= \left(\frac{2\pi^{p/2}}{p\Gamma(p/2)} \left(\frac{p(a_n-1)}{(a_n-p)} F_{1-\alpha,p,a_n-p} \right)^{p/2} |\Sigma_n|^{1/2} \right)^{1/p} + n^{1/2}s(n) \\ &\rightarrow (d_{\alpha,p} |\Sigma|^{1/2})^{1/p} > 0 \text{ w.p. 1 as } n \rightarrow \infty. \end{aligned} \tag{14}$$

By definition of $T^*(\epsilon)$

$$V(T^*(\epsilon) - 1) > \epsilon K_{T^*(\epsilon)-1}, \quad (15)$$

and there exists a random variable $Z(\epsilon)$ on $[0, 1]$ such that,

$$V(T^*(\epsilon) + Z(\epsilon)) \leq \epsilon K_{T^*(\epsilon)+Z(\epsilon)}. \quad (16)$$

Since K_n is strongly consistent for K and $T^*(\epsilon) \rightarrow \infty$ w.p. 1 as $\epsilon \rightarrow 0$,

$$K_{T^*(\epsilon)} \rightarrow K \quad \text{w.p. 1}, \quad (17)$$

Using (14), (15), (16), and (17)

$$\begin{aligned} \limsup_{\epsilon \rightarrow 0} \epsilon T^*(\epsilon)^{1/2} &\leq \limsup_{\epsilon \rightarrow 0} \frac{T^*(\epsilon)^{1/2} V(T^*(\epsilon) - 1)}{K_{T^*(\epsilon)-1}} = d_{\alpha,p}^{1/p} \frac{|\Sigma|^{1/2p}}{K} \quad \text{w.p. 1} \\ \liminf_{\epsilon \rightarrow 0} \epsilon T^*(\epsilon)^{1/2} &\geq \liminf_{\epsilon \rightarrow 0} \frac{T^*(\epsilon)^{1/2} V(T^*(\epsilon) + Z(\epsilon))}{K_{T^*(\epsilon)+Z(\epsilon)}} = d_{\alpha,p}^{1/p} \frac{|\Sigma|^{1/2p}}{K} \quad \text{w.p. 1.} \end{aligned}$$

Thus,

$$\lim_{\epsilon \rightarrow 0} \epsilon T^*(\epsilon)^{1/2} = d_{\alpha,p}^{1/p} \frac{|\Sigma|^{1/2p}}{K}. \quad (18)$$

Using (18) and the existence of a FCLT, by a standard random-time-change argument (Billingsley, 1968, p. 151)

$$\sqrt{T^*(\epsilon)} \Sigma_{T^*(\epsilon)}^{-1/2} (\theta_{T^*(\epsilon)} - \theta) \xrightarrow{d} N_p(0, I_p) \quad \text{as } \epsilon \rightarrow 0.$$

Finally,

$$\begin{aligned} &\Pr[\theta \in C_\alpha(T^*(\epsilon))] \\ &= \Pr \left[T^*(\epsilon) (\theta_{T^*(\epsilon)} - \theta)^T \Sigma_{T^*(\epsilon)}^{-1} (\theta_{T^*(\epsilon)} - \theta) \leq \frac{p(a_{T^*(\epsilon)} - 1)}{(a_{T^*(\epsilon)} - p)} F_{1-\alpha, p, a_{T^*(\epsilon)} - p; |\Sigma_{T^*(\epsilon)}| \neq 0} \right] \end{aligned}$$

$$\begin{aligned}
& + \Pr [\theta \in C_\alpha(T^*(\epsilon)); |\Sigma_{T^*(\epsilon)}| = 0] \\
& \rightarrow 1 - \alpha \text{ w.p. } 1 \text{ as } n \rightarrow \infty \text{ since } \Pr(|\Sigma_{T^*(\epsilon)}| = 0) \rightarrow 0 \text{ as } \epsilon \rightarrow 0.
\end{aligned}$$

C Proof of Theorem 2

Note that in this section we use the notation $|\cdot|$ to denote absolute value and not determinant. We first state the theorem more generally for processes that satisfy a strong invariance principle. Then, the proof of Theorem 2 will follow from Theorem 4 below and Corollary 5 in Vats et al. (2017).

Theorem 4. *Let Conditions 1 and 2 hold. If $b_n^{-1/2}(\log n)^{1/2}\gamma(n) \rightarrow 0$ as $n \rightarrow \infty$, then $\Sigma_n \rightarrow \Sigma$ w.p. 1 as $n \rightarrow \infty$.*

The proof of this theorem will be presented in a series of lemmas. We first construct $\tilde{\Sigma}$, a Brownian motion equivalent of the batch means estimator and show that $\tilde{\Sigma}$ converges to the identity matrix with probability 1 as n increases. This result will be critical in proving the theorem.

Let $B(t)$ be a p -dimensional standard Brownian motion, and for $i = 1, \dots, p$, let $B^{(i)}$ denote the i th component univariate Brownian motion. For $k = 0, \dots, a_n - 1$ define

$$\bar{B}_k^{(i)} = \frac{1}{b_n}(B^{(i)}((k+1)b_n) - B^{(i)}(kb_n)) \quad \text{and} \quad \bar{B}^{(i)}(n) = \frac{1}{n}B^{(i)}(n).$$

For $\bar{B}_k = (\bar{B}_k^{(1)}, \dots, \bar{B}_k^{(p)})^T$ and $\bar{B}(n) = (\bar{B}^{(1)}(n), \dots, \bar{B}^{(p)}(n))^T$, define

$$\tilde{\Sigma} = \frac{b_n}{a_n - 1} \sum_{k=0}^{a_n-1} [\bar{B}_k - \bar{B}(n)][\bar{B}_k - \bar{B}(n)]^T.$$

Here $\tilde{\Sigma}$ is the Brownian motion equivalent of Σ_n and in Lemma 3 we will show that $\tilde{\Sigma}$ converges to the identity matrix with probability 1. But first we state some results we will need.

Lemma 1 (Kendall and Stuart (1963)). *If $Z \sim \chi_v^2$, then for all positive integers r there exists a constant $K := K(r)$ such that $E[(Z - v)^{2r}] \leq Kv^r$.*

Lemma 2 (Billingsley (1968)). *Consider a family of random variables $\{R_n : n \geq 1\}$. If $E[|R_n|] \leq s_n$, where s_n is a sequence such that $\sum_n s_n < \infty$, then $R_n \rightarrow 0$ w.p. 1 as $n \rightarrow \infty$.*

Lemma 3. *If Condition 2 holds, then $\tilde{\Sigma} \rightarrow I_p$ with probability 1 as $n \rightarrow \infty$ where I_p is the $p \times p$ identity matrix.*

Proof. For $i, j = 1, \dots, p$, let $\tilde{\Sigma}_{ij}$ denote the (i, j) th component of $\tilde{\Sigma}$. For $i = j$, Damerджи (1994) showed that $\tilde{\Sigma}_{ij} \rightarrow 1$ with probability 1 as $n \rightarrow \infty$. Thus it is left to show that for $i \neq j$, $\tilde{\Sigma}_{ij} \rightarrow 0$ with probability 1 as $n \rightarrow \infty$.

$$\begin{aligned} \tilde{\Sigma}_{ij} &= \frac{b_n}{a_n - 1} \sum_{k=0}^{a_n-1} \left[\bar{B}_k^{(i)} - \bar{B}^{(i)}(n) \right] \left[\bar{B}_k^{(j)} - \bar{B}^{(j)}(n) \right] \\ &= \frac{b_n}{a_n - 1} \sum_{k=0}^{a_n-1} \left[\bar{B}_k^{(i)} \bar{B}_k^{(j)} - \bar{B}_k^{(i)} \bar{B}^{(j)}(n) - \bar{B}^{(i)}(n) \bar{B}_k^{(j)} + \bar{B}^{(i)}(n) \bar{B}^{(j)}(n) \right]. \end{aligned} \quad (19)$$

We will show that each of the four terms in (19) converges to 0 with probability 1 as $n \rightarrow \infty$. But first we note that by the properties of Brownian motion, for all $k = 0, \dots, a_n - 1$,

$$\begin{aligned} \bar{B}_k^{(i)} &\stackrel{iid}{\sim} N\left(0, \frac{1}{b_n}\right) \text{ and } \bar{B}_k^{(j)} \stackrel{iid}{\sim} N\left(0, \frac{1}{b_n}\right) \text{ independently} \\ &\Rightarrow \sqrt{b_n} \bar{B}_k^{(i)} \stackrel{iid}{\sim} N(0, 1) \text{ and } \sqrt{b_n} \bar{B}_k^{(j)} \stackrel{iid}{\sim} N(0, 1) \text{ independently.} \end{aligned} \quad (20)$$

1. Naturally by (20),

$$X_k := \sqrt{\frac{b_n}{2}} \bar{B}_k^{(i)} + \sqrt{\frac{b_n}{2}} \bar{B}_k^{(j)} \stackrel{iid}{\sim} N(0, 1) \text{ and } Y_k := \sqrt{\frac{b_n}{2}} \bar{B}_k^{(i)} - \sqrt{\frac{b_n}{2}} \bar{B}_k^{(j)} \stackrel{iid}{\sim} N(0, 1)$$

Notice that $AB = (A + B)^2/4 - (A - B)^2/4$. Using X_k as $(A + B)$ and Y_k as

($A - B$), we can write $b_n \bar{B}_k^{(i)} \bar{B}_k^{(j)}/2$ as a linear combination of two χ^2 random variables. Specifically,

$$\begin{aligned}
\frac{b_n}{a_n - 1} \sum_{k=0}^{a_n-1} \bar{B}_k^{(i)} \bar{B}_k^{(j)} &= \frac{2}{a_n - 1} \sum_{k=0}^{a_n-1} \sqrt{\frac{b_n}{2}} \bar{B}_k^{(i)} \sqrt{\frac{b_n}{2}} \bar{B}_k^{(j)} \\
&= \frac{1}{2(a_n - 1)} \sum_{k=0}^{a_n-1} [X_k^2 - Y_k^2] \\
&= \frac{1}{2(a_n - 1)} \sum_{k=0}^{a_n-1} X_k^2 - \frac{1}{2(a_n - 1)} \sum_{k=0}^{a_n-1} Y_k^2 \\
&= \frac{a_n}{2(a_n - 1)} \frac{X}{a_n} - \frac{a_n}{2(a_n - 1)} \frac{Y}{a_n}, \tag{21}
\end{aligned}$$

where $X = \sum_{k=0}^{a_n-1} X_k^2 \sim \chi_{a_n}^2$ and $Y = \sum_{k=0}^{a_n-1} Y_k^2 \sim \chi_{a_n}^2$ independently.

By Lemma 1, for all positive integers c ,

$$\mathbb{E} [(X - a_n)^{2c}] \leq K a_n^c \Rightarrow \mathbb{E} \left[\left(\frac{X}{a_n} - 1 \right)^{2c} \right] \leq K \left(\frac{b_n}{n} \right)^c.$$

Thus by Lemma 2 and Condition 22, $X/a_n \rightarrow 1$ with probability 1, as $n \rightarrow \infty$. Similarly, $Y/a_n \rightarrow 1$ with probability 1, as $n \rightarrow \infty$. Using this result in (21) and the fact that $a_n/(a_n - 1) \rightarrow 1$ as $n \rightarrow \infty$,

$$\frac{b_n}{a_n - 1} \sum_{k=0}^{a_n-1} \bar{B}_k^{(i)} \bar{B}_k^{(j)} \rightarrow 0 \text{ w.p. } 1 \text{ as } n \rightarrow \infty.$$

2. By the definition of $\bar{B}(n)$ and \bar{B}_k ,

$$\begin{aligned}
\frac{b_n}{a_n - 1} \sum_{k=0}^{a_n-1} \bar{B}_k^{(i)} \bar{B}_k^{(j)}(n) &= \frac{1}{a_n - 1} \frac{1}{n} B^{(j)}(n) \sum_{k=0}^{a_n-1} B^{(i)}((k+1)b_n) - B^{(i)}(kb_n) \\
&= \frac{1}{a_n - 1} \frac{1}{n} B^{(j)}(n) B^{(i)}(a_n b_n) \\
&= \frac{a_n}{a_n - 1} \frac{\sqrt{b_n}}{n} B^{(j)}(n) \frac{\sqrt{b_n}}{a_n b_n} B^{(i)}(a_n b_n). \tag{22}
\end{aligned}$$

Using properties of Brownian motion,

$$\begin{aligned} B^{(j)}(n) &\sim N(0, n) \quad \text{and} \quad B^{(i)}(a_n b_n) \sim N(0, a_n b_n) \\ \Rightarrow \frac{\sqrt{b_n}}{n} B^{(j)}(n) &\stackrel{d}{\sim} N\left(0, \frac{b_n}{n}\right) \quad \text{and} \quad \frac{\sqrt{b_n}}{a_n b_n} B^{(i)}(a_n b_n) \stackrel{d}{\sim} N\left(0, \frac{1}{a_n}\right). \end{aligned} \quad (23)$$

As $n \rightarrow \infty$ both terms in (23) tend to Dirac's delta function. Thus as $n \rightarrow \infty$.

$$\frac{\sqrt{b_n}}{n} B^{(j)}(n) \rightarrow 0 \text{ w.p. } 1 \quad \text{and} \quad \frac{\sqrt{b_n}}{a_n b_n} B^{(i)}(a_n b_n) \rightarrow 0 \text{ w.p. } 1. \quad (24)$$

Using (24) in (22),

$$\frac{b_n}{a_n - 1} \sum_{k=0}^{a_n-1} \bar{B}_k^{(i)} \bar{B}_k^{(j)}(n) \rightarrow 0 \text{ w.p. } 1 \text{ as } n \rightarrow \infty.$$

3. A similar argument as above yields,

$$\frac{b_n}{a_n - 1} \sum_{k=0}^{a_n-1} \bar{B}^{(i)}(n) \bar{B}_k^{(j)} \rightarrow 0 \text{ w.p. } 1 \text{ as } n \rightarrow \infty.$$

4. By the definition of $\bar{B}^{(i)}(n)$,

$$\begin{aligned} \frac{b_n}{a_n - 1} \sum_{k=0}^{a_n-1} \bar{B}^{(i)}(n) \bar{B}^{(j)}(n) &= \frac{b_n}{a_n - 1} a_n \frac{1}{n} B^{(i)}(n) \frac{1}{n} B^{(j)}(n) \\ &= \frac{a_n}{a_n - 1} \frac{\sqrt{b_n}}{n} B^{(i)}(n) \frac{\sqrt{b_n}}{n} B^{(j)}(n) \\ &\rightarrow 0 \text{ w.p. } 1 \text{ as } n \rightarrow \infty \text{ by (24)}. \end{aligned}$$

Thus each term in (19) goes to 0 with probability 1 as $n \rightarrow \infty$, yielding $\tilde{\Sigma} \rightarrow I_p$ with probability 1 as $n \rightarrow \infty$. \square

Corollary 1. *If Condition 2 holds, then for any conformable matrix L , as $n \rightarrow \infty$,*

$L\tilde{\Sigma}L^T \rightarrow LL^T$ with probability 1.

For the rest of the proof, we will require some results regarding Brownian motion.

Lemma 4 (Csörgő and Révész (1981)). *Suppose Condition 21 holds, then for all $\epsilon > 0$ and for almost all sample paths, there exists $n_0(\epsilon)$ such that for all $n \geq n_0$ and all $i = 1, \dots, p$*

$$\sup_{0 \leq t \leq n-b_n} \sup_{0 \leq s \leq b_n} |B^{(i)}(t+s) - B^{(i)}(t)| < (1+\epsilon) \left(2b_n \left(\log \frac{n}{b_n} + \log \log n \right) \right)^{1/2}$$

$$\sup_{0 \leq s \leq b_n} |B^{(i)}(n) - B^{(i)}(n-s)| < (1+\epsilon) \left(2b_n \left(\log \frac{n}{b_n} + \log \log n \right) \right)^{1/2}$$

and

$$|B^{(i)}(n)| < (1+\epsilon) \sqrt{2n \log \log n}.$$

Corollary 2 (Damerджи (1994)). *Suppose Condition 21 holds, then for all $\epsilon > 0$ and for almost all sample paths, there exists $n_0(\epsilon)$ such that for all $n \geq n_0$ and all $i = 1, \dots, p$*

$$|\bar{B}_k^{(i)}(b_n)| \leq \frac{\sqrt{2}}{\sqrt{b_n}} (1+\epsilon) \left(\log \frac{n}{b_n} + \log \log n \right)^{1/2}.$$

Recall L in (11) and set $\Sigma := LL^T$. Define $C(t) = LB(t)$ and if $C^{(i)}(t)$ is the i th component of $C(t)$, define

$$\bar{C}_k^{(i)} := \frac{1}{b_n} \left(C^{(i)}((k+1)b_n) - C^{(i)}(kb_n) \right) \quad \text{and} \quad \bar{C}^{(i)}(n) := \frac{1}{n} C^{(i)}(n).$$

Since $C^{(i)}(t) \sim N(0, t\Sigma_{ii})$, where Σ_{ii} is the i th diagonal of Σ , $C^{(i)}/\sqrt{\Sigma_{ii}}$ is a 1-dimensional Brownian motion. As a consequence, we have the following corollaries of Lemma 4.

Corollary 3. *For all $\epsilon > 0$ and for almost all sample paths there exists $n_0(\epsilon)$ such that*

for all $n \geq n_0$ and all $i = 1, \dots, p$

$$\left| C^{(i)}(n) \right| < (1 + \epsilon) [2\Sigma_{ii}n \log \log n]^{1/2},$$

where Σ_{ii} is the i th diagonal of Σ .

Corollary 4. For all $\epsilon > 0$ and for almost all sample paths, there exists $n_0(\epsilon)$ such that for all $n \geq n_0$ and all $i = 1, \dots, p$

$$\left| \bar{C}_k^{(i)} \right| \leq \sqrt{\frac{2\Sigma_{ii}}{b_n}} (1 + \epsilon) \left(\log \frac{n}{b_n} + \log \log n \right)^{1/2},$$

where Σ_{ii} is the i th diagonal of Σ .

We finally come to the last leg of the proof, where we will show that for the (i, j) th element of Σ_n , $|\Sigma_{n,ij} - \Sigma_{ij}| \rightarrow 0$ with probability 1 as $n \rightarrow \infty$.

Recall $Y_t = g(X_t)$. Let $Y_t^{(i)}$ be the i th component of Y_t . Define for each $i = 1, \dots, p$, the process $V_l^{(i)} = Y_l^{(i)} - \theta_i$ for $l = 1, 2, \dots$. Further, for $k = 0, \dots, a_n - 1$ and $j = 1, \dots, p$ define

$$\bar{V}_k^{(i)} = \frac{1}{b_n} \sum_{l=1}^{b_n} V_{kb_n+l}^{(i)} \quad \text{and} \quad \bar{V}^{(i)}(n) = \frac{1}{n} \sum_{l=1}^n V_l^{(i)}.$$

Then

$$\Sigma_{n,ij} = \frac{b_n}{a_n - 1} \sum_{k=0}^{a_n-1} \left[\bar{V}_k^{(i)} - \bar{V}^{(i)}(n) \right] \left[\bar{V}_k^{(j)} - \bar{V}^{(j)}(n) \right].$$

We will show that $|\Sigma_{n,ij} - \Sigma_{ij}| \rightarrow 0$ w.p. 1 as $n \rightarrow \infty$.

$$\begin{aligned} & |\Sigma_{n,ij} - \Sigma_{ij}| \\ &= \left| \frac{b_n}{a_n - 1} \sum_{k=0}^{a_n-1} \left[\bar{V}_k^{(i)} - \bar{V}^{(i)}(n) \right] \left[\bar{V}_k^{(j)} - \bar{V}^{(j)}(n) \right] - \Sigma_{ij} \right| \\ &= \left| \frac{b_n}{a_n - 1} \sum_{k=0}^{a_n-1} \left[\bar{V}_k^{(i)} - \bar{V}^{(i)}(n) \pm \bar{C}_k^{(i)} \pm \bar{C}^{(i)}(n) \right] \left[\bar{V}_k^{(j)} - \bar{V}^{(j)}(n) \pm \bar{C}_k^{(j)} \pm \bar{C}^{(j)}(n) \right] - \Sigma_{ij} \right| \end{aligned}$$

$$\begin{aligned}
&= \left| \frac{b_n}{a_n - 1} \sum_{k=0}^{a_n-1} \left[\left(\bar{V}_k^{(i)} - \bar{C}_k^{(i)} \right) - \left(\bar{V}^{(i)}(n) - \bar{C}^{(i)}(n) \right) + \left(\bar{C}_k^{(i)} - \bar{C}^{(i)}(n) \right) \right] \right. \\
&\quad \left. \left[\left(\bar{V}_k^{(j)} - \bar{C}_k^{(j)} \right) - \left(\bar{V}^{(j)}(n) - \bar{C}^{(j)}(n) \right) + \left(\bar{C}_k^{(j)} - \bar{C}^{(j)}(n) \right) \right] - \Sigma_{ij} \right| \\
&\leq \left| \frac{b_n}{a_n - 1} \sum_{k=0}^{a_n-1} \left[\bar{C}_k^{(i)} - \bar{C}^{(i)}(n) \right] \left[\bar{C}_k^{(j)} - \bar{C}^{(j)}(n) \right] - \Sigma_{ij} \right| \\
&+ \frac{b_n}{a_n - 1} \sum_{k=0}^{a_n-1} \left[\left| \left(\bar{V}_k^{(i)} - \bar{C}_k^{(i)} \right) \left(\bar{V}_k^{(j)} - \bar{C}_k^{(j)} \right) \right| \right. \\
&+ \left| \left(\bar{V}^{(i)}(n) - \bar{C}^{(i)}(n) \right) \left(\bar{V}^{(j)}(n) - \bar{C}^{(j)}(n) \right) \right| \\
&+ \left| \left(\bar{V}_k^{(i)} - \bar{C}_k^{(i)} \right) \left(\bar{V}^{(j)}(n) - \bar{C}^{(j)}(n) \right) \right| + \left| \left(\bar{V}^{(i)}(n) - \bar{C}^{(i)}(n) \right) \left(\bar{V}_k^{(j)} - \bar{C}_k^{(j)} \right) \right| \\
&+ \left| \left(\bar{V}_k^{(i)} - \bar{C}_k^{(i)} \right) \bar{C}_k^{(j)} \right| + \left| \left(\bar{V}_k^{(j)} - \bar{C}_k^{(j)} \right) \bar{C}_k^{(i)} \right| \\
&+ \left| \left(\bar{V}_k^{(i)} - \bar{C}_k^{(i)} \right) \bar{C}^{(j)}(n) \right| + \left| \left(\bar{V}_k^{(j)} - \bar{C}_k^{(j)} \right) \bar{C}^{(i)}(n) \right| \\
&+ \left| \left(\bar{V}^{(i)}(n) - \bar{C}^{(i)}(n) \right) \bar{C}_k^{(j)} \right| + \left| \left(\bar{V}^{(j)}(n) - \bar{C}^{(j)}(n) \right) \bar{C}_k^{(i)} \right| \\
&+ \left. \left| \left(\bar{V}^{(i)}(n) - \bar{C}^{(i)}(n) \right) \bar{C}^{(j)}(n) \right| + \left| \left(\bar{V}^{(j)}(n) - \bar{C}^{(j)}(n) \right) \bar{C}^{(i)}(n) \right| \right].
\end{aligned}$$

We will show that each of the 13 terms above tends to 0 w.p. 1 as $n \rightarrow \infty$.

1. Notice that,

$$\frac{b_n}{a_n - 1} \sum_{k=0}^{a_n-1} \left[\bar{C}_k^{(i)} - \bar{C}^{(i)}(n) \right] \left[\bar{C}_k^{(j)} - \bar{C}^{(j)}(n) \right],$$

is the (i, j) th entry in $L\tilde{\Sigma}L^T$. Thus, by Corollary 1, with probability 1 as $n \rightarrow \infty$,

$$\left| \frac{b_n}{a_n - 1} \sum_{k=0}^{a_n-1} \left[\bar{C}_k^{(i)} - \bar{C}^{(i)}(n) \right] \left[\bar{C}_k^{(j)} - \bar{C}^{(j)}(n) \right] - \Sigma_{ij} \right| \rightarrow 0.$$

2. By Condition 1

$$\left\| \sum_{l=0}^n V_l - LB(n) \right\| < D\gamma(n) \text{ w.p. } 1,$$

where $V_l = (V_l^{(1)}, \dots, V_l^{(p)})$. Hence, for components i and j

$$\left| \sum_{l=1}^n V_l^{(i)} - C^{(i)}(n) \right| < D\gamma(n) \quad \text{and} \quad \left| \sum_{l=1}^n V_l^{(j)} - C^{(j)}(n) \right| < D\gamma(n). \quad (25)$$

Note that,

$$\begin{aligned} \left| \bar{V}_k^{(i)} - \bar{C}_k^{(i)} \right| &= \left| \frac{1}{b_n} \left[\sum_{l=1}^{(k+1)b_n} V_l^{(i)} - C^{(i)}((k+1)b_n) \right] - \frac{1}{b_n} \left[\sum_{l=1}^{kb_n} V_l^{(i)} - C^{(i)}(kb_n) \right] \right| \\ &\leq \frac{1}{b_n} \left[\left| \sum_{l=1}^{(k+1)b_n} V_l^{(i)} - C^{(i)}((k+1)b_n) \right| + \left| \sum_{l=1}^{kb_n} V_l^{(i)} - C^{(i)}(kb_n) \right| \right] \\ &\leq \frac{2}{b_n} D\gamma(n). \end{aligned} \quad (26)$$

Similarly

$$\left| \bar{V}_k^{(j)} - \bar{C}_k^{(j)} \right| \leq \frac{2}{b_n} D\gamma(n). \quad (27)$$

Thus, using (26) and (27),

$$\begin{aligned} \frac{b_n}{a_n - 1} \sum_{k=0}^{a_n-1} \left| \left(\bar{V}_k^{(i)} - \bar{C}_k^{(i)} \right) \left(\bar{V}_k^{(j)} - \bar{C}_k^{(j)} \right) \right| &\leq \frac{b_n}{a_n - 1} a_n \frac{4D^2}{b_n^2} \gamma(n)^2 \\ &\leq 4D^2 \frac{a_n}{a_n - 1} \frac{\log n}{b_n} \gamma(n)^2 \\ &\rightarrow 0 \text{ w.p } 1 \text{ as } n \rightarrow \infty. \end{aligned}$$

3. By (25), we get

$$\left| \bar{V}^{(i)}(n) - \bar{C}^{(i)}(n) \right| = \frac{1}{n} \left| \sum_{l=1}^n V_l^{(i)} - C^{(i)}(n) \right| < D \frac{\gamma(n)}{n}. \quad (28)$$

Similarly ,

$$\left| \bar{V}^{(j)}(n) - \bar{C}^{(j)}(n) \right| < D \frac{\gamma(n)}{n}. \quad (29)$$

Then,

$$\begin{aligned}
& \frac{b_n}{a_n - 1} \sum_{k=0}^{a_n-1} \left| \left(\bar{V}^{(i)}(n) - \bar{C}^{(i)}(n) \right) \left(\bar{V}^{(j)}(n) - \bar{C}^{(j)}(n) \right) \right| \\
& < \frac{b_n}{a_n - 1} a_n D^2 \frac{\gamma(n)^2}{n^2} \\
& = D^2 \frac{a_n}{a_n - 1} \frac{b_n}{n} \frac{b_n}{n} \frac{\gamma(n)^2}{b_n} \\
& < D^2 \frac{a_n}{a_n - 1} \frac{b_n}{n} \frac{b_n}{n} \frac{\gamma(n)^2 \log n}{b_n} \\
& \rightarrow 0 \text{ w.p. } 1 \text{ as } n \rightarrow \infty \text{ by Condition 21.}
\end{aligned}$$

4. By (26) and (29), we have

$$\begin{aligned}
& \frac{b_n}{a_n - 1} \sum_{k=0}^{a_n-1} \left| \left(\bar{V}_k^{(i)} - \bar{C}_k^{(i)} \right) \left(\bar{V}^{(j)}(n) - \bar{C}^{(j)}(n) \right) \right| \\
& \leq \frac{b_n}{a_n - 1} a_n \left(\frac{2D}{b_n} \gamma(n) \right) \left(\frac{D}{n} \gamma(n) \right) \\
& < 2D^2 \frac{a_n}{a_n - 1} \frac{b_n}{n} \frac{\gamma(n)^2 \log n}{b_n} \\
& \rightarrow 0 \text{ w.p. } 1 \text{ as } n \rightarrow \infty \text{ by Condition 21.}
\end{aligned}$$

5. By (27) and (28), we have

$$\begin{aligned}
& \frac{b_n}{a_n - 1} \sum_{k=0}^{a_n-1} \left| \left(\bar{V}^{(i)}(n) - \bar{C}^{(i)}(n) \right) \left(\bar{V}_k^{(j)} - \bar{C}_k^{(j)} \right) \right| \\
& \leq \frac{b_n}{a_n - 1} a_n \left(\frac{2D}{b_n} \gamma(n) \right) \left(\frac{D}{n} \gamma(n) \right) \\
& < 2D^2 \frac{a_n}{a_n - 1} \frac{b_n}{n} \frac{\gamma(n)^2 \log n}{b_n} \\
& \rightarrow 0 \text{ w.p. } 1 \text{ as } n \rightarrow \infty \text{ by Condition 21.}
\end{aligned}$$

6. By Corollary 4 and (26)

$$\begin{aligned}
& \frac{b_n}{a_n - 1} \sum_{k=0}^{a_n-1} \left| \left(\bar{V}_k^{(i)} - \bar{C}_k^{(i)} \right) \bar{C}_k^{(j)} \right| \\
& < \frac{b_n}{a_n - 1} a_n \left(\frac{2D}{b_n} \gamma(n) \right) \left(\sqrt{\frac{2\Sigma_{ii}}{b_n}} (1 + \epsilon) \left(\log \frac{n}{b_n} + \log \log n \right)^{1/2} \right) \\
& < 2^{3/2} \Sigma_{ii}^{1/2} D (1 + \epsilon) \frac{a_n}{a_n - 1} \frac{\gamma(n)}{\sqrt{b_n}} (2 \log n)^{1/2} \\
& \rightarrow 0 \text{ w.p. } 1 \text{ as } n \rightarrow \infty \text{ by Condition 21.}
\end{aligned}$$

7. By Corollary 4 and (27)

$$\begin{aligned}
& \frac{b_n}{a_n - 1} \sum_{k=0}^{a_n-1} \left| \left(\bar{V}_k^{(j)} - \bar{C}_k^{(j)} \right) \bar{C}_k^{(i)} \right| \\
& < \frac{b_n}{a_n - 1} a_n \left(\frac{2D}{b_n} \gamma(n) \right) \left(\sqrt{\frac{2\Sigma_{ii}}{b_n}} (1 + \epsilon) \left(\log \frac{n}{b_n} + \log \log n \right)^{1/2} \right) \\
& < 2^{3/2} \Sigma_{ii}^{1/2} D (1 + \epsilon) \frac{a_n}{a_n - 1} \frac{\gamma(n)}{\sqrt{b_n}} (2 \log n)^{1/2} \\
& \rightarrow 0 \text{ w.p. } 1 \text{ as } n \rightarrow \infty \text{ by Condition 21.}
\end{aligned}$$

8. By Corollary 3 and (26)

$$\begin{aligned}
& \frac{b_n}{a_n - 1} \sum_{k=0}^{a_n-1} \left| \left(\bar{V}_k^{(i)} - \bar{C}_k^{(i)} \right) \bar{C}_k^{(j)}(n) \right| \\
& < \frac{b_n}{a_n - 1} a_n \left(\frac{2D}{b_n} \gamma(n) \right) \left(\frac{1}{n} (1 + \epsilon) (2\Sigma_{ii} n \log \log n)^{1/2} \right) \\
& < 2^{3/2} D \sqrt{\Sigma_{ii}} (1 + \epsilon) \frac{a_n}{a_n - 1} \frac{\gamma(n) (\log n)^{1/2}}{n^{1/2}} \\
& = 2^{3/2} D \sqrt{\Sigma_{ii}} (1 + \epsilon) \frac{a_n}{a_n - 1} \left(\frac{b_n}{n} \right)^{1/2} \frac{\gamma(n) (\log n)^{1/2}}{b_n^{1/2}} \\
& \rightarrow 0 \text{ w.p. } 1 \text{ as } n \rightarrow \infty \text{ by Condition 21.}
\end{aligned}$$

9. By Corollary 3 and (27)

$$\begin{aligned}
& \frac{b_n}{a_n - 1} \sum_{k=0}^{a_n-1} \left| \left(\bar{V}_k^{(j)} - \bar{C}_k^{(j)} \right) \bar{C}^{(i)}(n) \right| \\
& < \frac{b_n}{a_n - 1} a_n \left(\frac{2D}{b_n} \gamma(n) \right) \left(\frac{1}{n} (1 + \epsilon) (2\Sigma_{ii} n \log \log n)^{1/2} \right) \\
& < 2^{3/2} D \sqrt{\Sigma_{ii}} (1 + \epsilon) \frac{a_n}{a_n - 1} \frac{\gamma(n) (\log n)^{1/2}}{n^{1/2}} \\
& = 2^{3/2} D \sqrt{\Sigma_{ii}} (1 + \epsilon) \frac{a_n}{a_n - 1} \left(\frac{b_n}{n} \right)^{1/2} \frac{\gamma(n) (\log n)^{1/2}}{b_n^{1/2}} \\
& \rightarrow 0 \text{ w.p. } 1 \text{ as } n \rightarrow \infty \text{ by Condition 21.}
\end{aligned}$$

10. By (28) and Corollary 4

$$\begin{aligned}
& \frac{b_n}{a_n - 1} \sum_{k=0}^{a_n-1} \left| \left(\bar{V}^{(i)}(n) - \bar{C}^{(i)}(n) \right) \bar{C}_k^{(j)} \right| \\
& < \frac{b_n}{a_n - 1} a_n \left(\frac{D}{n} \gamma(n) \right) \left(\sqrt{\frac{2\Sigma_{ii}}{b_n}} (1 + \epsilon) \left(\log \frac{n}{b_n} + \log \log n \right)^{1/2} \right) \\
& < \sqrt{2\Sigma_{ii}} D (1 + \epsilon) \frac{a_n}{a_n - 1} \frac{b_n}{n} \gamma(n) \left(\frac{2}{b_n} \log n \right)^{1/2} \\
& = 2^{3/2} \Sigma_{ii}^{1/2} D (1 + \epsilon) \frac{a_n}{a_n - 1} \frac{b_n}{n} \frac{\gamma(n) (\log n)^{1/2}}{b_n^{1/2}} \\
& \rightarrow 0 \text{ w.p. } 1 \text{ as } n \rightarrow \infty \text{ by Condition 21.}
\end{aligned}$$

11. By (29) and Corollary 4

$$\begin{aligned}
& \frac{b_n}{a_n - 1} \sum_{k=0}^{a_n-1} \left| \left(\bar{V}^{(j)}(n) - \bar{C}^{(j)}(n) \right) \bar{C}_k^{(i)} \right| \\
& < \frac{b_n}{a_n - 1} a_n \left(D \frac{\gamma(n)}{n} \right) \left(\sqrt{\frac{2\Sigma_{ii}}{b_n}} (1 + \epsilon) \left(\log \frac{n}{b_n} + \log \log n \right)^{1/2} \right) \\
& < \sqrt{2\Sigma_{ii}} D (1 + \epsilon) \frac{a_n}{a_n - 1} \frac{b_n}{n} \gamma(n) \left(\frac{2}{b_n} \log n \right)^{1/2}
\end{aligned}$$

$$\begin{aligned}
&= 2^{3/2} \Sigma_{ii}^{1/2} D(1 + \epsilon) \frac{a_n}{a_n - 1} \frac{b_n}{n} \frac{\gamma(n)(\log n)^{1/2}}{b_n^{1/2}} \\
&\rightarrow 0 \text{ w.p. } 1 \text{ as } n \rightarrow \infty \text{ by Condition 21.}
\end{aligned}$$

12. By (28) and Corollary 3

$$\begin{aligned}
&\frac{b_n}{a_n - 1} \sum_{k=0}^{a_n-1} \left| \left(\bar{V}^{(i)}(n) - \bar{C}^{(i)}(n) \right) \bar{C}^{(j)}(n) \right| \\
&< \frac{b_n}{a_n - 1} a_n \left(\frac{D}{n} \gamma(n) \right) \left(\frac{1}{n} (1 + \epsilon) (2 \Sigma_{ii} n \log \log n)^{1/2} \right) \\
&< \sqrt{2 \Sigma_{ii}} D(1 + \epsilon) \frac{a_n}{a_n - 1} \frac{b_n}{n} \frac{\gamma(n)(\log n)^{1/2}}{n^{1/2}} \\
&\rightarrow 0 \text{ w.p. } 1 \text{ as } n \rightarrow \infty \text{ by Condition 21.}
\end{aligned}$$

13. By (29) and Corollary 3

$$\begin{aligned}
&\frac{b_n}{a_n - 1} \sum_{k=0}^{a_n-1} \left| \left(\bar{V}^{(j)}(n) - \bar{C}^{(j)}(n) \right) \bar{C}^{(i)}(n) \right| \\
&< \frac{b_n}{a_n - 1} a_n \left(D \frac{\gamma(n)}{n} \right) \left(\frac{1}{n} (1 + \epsilon) (2 \Sigma_{ii} n \log \log n)^{1/2} \right) \\
&< \sqrt{2 \Sigma_{ii}} D(1 + \epsilon) \frac{a_n}{a_n - 1} \frac{b_n}{n} \frac{\gamma(n)(\log n)^{1/2}}{n^{1/2}} \\
&\rightarrow 0 \text{ w.p. } 1 \text{ as } n \rightarrow \infty \text{ by Condition 21.}
\end{aligned}$$

Thus, each of the 13 terms tends to 0 with probability 1 as $n \rightarrow \infty$, giving that $\Sigma_{n,ij} \rightarrow \Sigma_{ij}$ w.p. 1 as $n \rightarrow \infty$.

D Proof of Theorem 3

Without loss of generality, we assume $\tau^2 = 1$. The posterior distribution for this Bayesian logistic regression model is,

$$\begin{aligned} f(\beta|y, x) &\propto f(\beta) \prod_{i=1}^K f(y_i|x_i, \beta) \\ &\propto e^{-\frac{1}{2}\beta^T\beta} \prod_{i=1}^K \left(\frac{1}{1 + e^{-x_i\beta}} \right)^{y_i} \left(\frac{e^{-x_i\beta}}{1 + e^{-x_i\beta}} \right)^{1-y_i}. \end{aligned} \quad (30)$$

For simpler notation we will use $f(\beta)$ to denote the posterior density. Note that the posterior has a moment generating function.

Consider a random walk Metropolis-Hastings algorithm with a multivariate normal proposal distribution to sample from the posterior $f(\beta)$. We will use the following result to establish geometric ergodicity of this Markov chain.

Theorem 5 (Jarner and Hansen (2000)). *Let $m(\beta) = \nabla f(\beta)/\|\nabla f(\beta)\|$ and also let $n(\beta) = \beta/\|\beta\|$. Suppose f on \mathbb{R}^p is super-exponential in that it is positive and has continuous first derivatives such that*

$$\lim_{\|\beta\| \rightarrow \infty} n(\beta) \cdot \nabla \log f(\beta) = -\infty. \quad (31)$$

In addition let the proposal distribution be bounded away from 0 in some region around zero. If

$$\limsup_{\|\beta\| \rightarrow \infty} n(\beta) \cdot m(\beta) < 0, \quad (32)$$

then the random walk Metropolis-Hastings algorithm is geometrically ergodic.

Proof of Theorem 3. Note that the multivariate normal proposal distribution q is indeed bounded away from zero in some region around zero. We will first show that f is super-exponential. It is easy to see that f has continuous first derivatives and is positive. Next

we need to establish (31). From (30) we see that

$$\begin{aligned}
& \log f(\beta) \\
&= \text{const} - \frac{1}{2} \beta^T \beta - \sum_{i=1}^K y_i \log(1 + e^{-x_i \beta}) - \sum_{i=1}^K (1 - y_i) x_i \beta - \sum_{i=1}^K (1 - y_i) \log(1 + e^{-x_i \beta}) \\
&= \text{const} - \frac{1}{2} \beta^T \beta - \sum_{i=1}^K \log(1 + e^{-x_i \beta}) - \sum_{i=1}^K (1 - y_i) x_i \beta \\
&= \text{const} - \frac{1}{2} \sum_{j=1}^p \beta_j^2 - \sum_{i=1}^K \log(1 + e^{-\sum_{j=1}^p x_{ij} \beta_j}) - \sum_{i=1}^K (1 - y_i) \sum_{j=1}^p x_{ij} \beta_j.
\end{aligned}$$

For $l = 1, \dots, p$

$$\frac{\partial \log f(\beta)}{\partial \beta_l} = -\beta_l + \sum_{i=1}^K \frac{x_{il} e^{-x_i \beta}}{1 + e^{-x_i \beta}} - \sum_{i=1}^K (1 - y_i) x_{il}$$

and

$$\begin{aligned}
\beta \cdot \nabla \log f(\beta) &= \sum_{j=1}^p \left[-\beta_j^2 + \sum_{i=1}^K x_{ij} \beta_j \frac{e^{-x_i \beta}}{1 + e^{-x_i \beta}} - \sum_{i=1}^K (1 - y_i) x_{ij} \beta_j \right] \\
&= -\|\beta\|^2 + \sum_{i=1}^K x_i \beta \frac{e^{-x_i \beta}}{1 + e^{-x_i \beta}} - \sum_{i=1}^K (1 - y_i) x_i \beta.
\end{aligned}$$

Hence

$$\frac{\beta}{\|\beta\|} \cdot \nabla \log f(\beta) = -\|\beta\| + \sum_{i=1}^K \frac{x_i \beta}{\|\beta\|} \frac{e^{-x_i \beta}}{1 + e^{-x_i \beta}} - \sum_{i=1}^K (1 - y_i) \frac{x_i \beta}{\|\beta\|}.$$

Taking the limit with $\|\beta\| \rightarrow \infty$ we obtain

$$\begin{aligned}
\lim_{\|\beta\| \rightarrow \infty} \frac{\beta}{\|\beta\|} \cdot \nabla \log f(\beta) &= - \lim_{\|\beta\| \rightarrow \infty} \|\beta\| + \lim_{\|\beta\| \rightarrow \infty} \sum_{i=1}^K \frac{x_i \beta}{\|\beta\|} \frac{e^{-x_i \beta}}{1 + e^{-x_i \beta}} \\
&\quad - \lim_{\|\beta\| \rightarrow \infty} \sum_{i=1}^K (1 - y_i) \frac{x_i \beta}{\|\beta\|}. \tag{33}
\end{aligned}$$

By the Cauchy-Schwarz inequality we can bound the second term

$$\lim_{\|\beta\| \rightarrow \infty} \sum_{i=1}^K \frac{x_i \beta}{\|\beta\|} \frac{e^{-x_i \beta}}{1 + e^{-x_i \beta}} \leq \lim_{\|\beta\| \rightarrow \infty} \sum_{i=1}^K \frac{|x_i| \|\beta\|}{\|\beta\|} \frac{e^{-x_i \beta}}{1 + e^{-x_i \beta}} \leq \sum_{i=1}^K |x_i|. \quad (34)$$

For the third term we obtain

$$\begin{aligned} \lim_{\|\beta\| \rightarrow \infty} \sum_{i=1}^K (1 - y_i) \frac{x_i \beta}{\|\beta\|} &= \lim_{\|\beta\| \rightarrow \infty} \sum_{i=1}^K (1 - y_i) \frac{\sum_{j=1}^p x_{ij} \beta_j}{\|\beta\|} \\ &= \sum_{i=1}^K (1 - y_i) \sum_{j=1}^p \lim_{\|\beta\| \rightarrow \infty} \frac{x_{ij} \beta_j}{\|\beta\|} \\ &\geq \sum_{i=1}^K (1 - y_i) \sum_{j=1}^p \lim_{\|\beta\| \rightarrow \infty} \frac{-|x_{ij}| |\beta_j|}{\|\beta\|} \\ &\geq - \sum_{i=1}^K (1 - y_i) \sum_{j=1}^p \lim_{\|\beta\| \rightarrow \infty} |x_{ij}| \quad \text{Since } |\beta_j| \leq \|\beta\| \\ &= - \sum_{i=1}^K (1 - y_i) \|x_i\|_1. \end{aligned} \quad (35)$$

Using (34) and (35) in (33).

$$\lim_{\|\beta\| \rightarrow \infty} \frac{\beta}{\|\beta\|} \cdot \nabla \log f(\beta) \leq - \lim_{\|\beta\| \rightarrow \infty} \|\beta\| + \sum_{i=1}^K |x_i| + \sum_{i=1}^K (1 - y_i) \|x_i\|_1 = -\infty.$$

Next we need to establish (32). Notice that

$$f(\beta) \propto \exp \left[-\frac{1}{2} \sum_{j=1}^p \beta_j^2 - \sum_{i=1}^K (1 - y_i) \sum_{j=1}^p x_{ij} \beta_j - \sum_{i=1}^K \log(1 + e^{-\sum_{j=1}^p x_{ij} \beta_j}) \right] := e^{C(\beta)}$$

and hence for $l = 1, \dots, p$

$$\frac{\partial f(\beta)}{\partial \beta_l} = e^{C(\beta)} \left[-\beta_l - \sum_{i=1}^K (1 - y_i) x_{il} - \sum_{i=1}^K \frac{-x_{il} e^{-x_i \beta}}{1 + e^{-x_i \beta}} \right].$$

In order to show the result, we will need evaluate

$$\lim_{\|\beta\| \rightarrow \infty} \frac{e^{C(\beta)\|\beta\|}}{\|\nabla f(\beta)\|}.$$

To this end, we will first show that

$$\lim_{\|\beta\| \rightarrow \infty} \frac{\|\nabla f(\beta)\|^2}{e^{2C(\beta)\|\beta\|^2}} = 1.$$

We calculate that

$$\begin{aligned} & \|\nabla f(\beta)\|^2 \\ &= e^{2C(\beta)} \sum_{j=1}^p \left[-\beta_j - \sum_{i=1}^K (1-y_i)x_{ij} + \sum_{i=1}^K \frac{x_{ij}e^{-x_i\beta}}{1+e^{-x_i\beta}} \right]^2 \\ &= e^{2C(\beta)} \sum_{j=1}^p \left[\left(\sum_{i=1}^K \frac{x_{ij}e^{-x_i\beta}}{1+e^{-x_i\beta}} \right)^2 + \beta_j^2 + \left(\sum_{i=1}^K (1-y_i)x_{ij} \right)^2 + 2 \sum_{i=1}^K (1-y_i)x_{ij}\beta_j \right. \\ &\quad \left. - 2 \left(\beta_j + \sum_{i=1}^K (1-y_i)x_{ij} \right) \left(\sum_{i=1}^K x_{ij} \frac{e^{-x_i\beta}}{1+e^{-x_i\beta}} \right) \right] \\ &= e^{2C(\beta)} \left[\sum_{j=1}^p \left(\sum_{i=1}^K \frac{x_{ij}e^{-x_i\beta}}{1+e^{-x_i\beta}} \right)^2 + \|\beta\|^2 + \sum_{j=1}^p \left(\sum_{i=1}^K (1-y_i)x_{ij} \right)^2 + 2 \sum_{i=1}^K (1-y_i)x_i\beta \right. \\ &\quad \left. - 2 \sum_{i=1}^K x_i\beta \frac{e^{-x_i\beta}}{1+e^{-x_i\beta}} - 2 \sum_{j=1}^p \left(\sum_{i=1}^K (1-y_i)x_i \right) \left(\sum_{i=1}^K x_{ij} \frac{e^{-x_i\beta}}{1+e^{-x_i\beta}} \right) \right] \\ &= e^{2C(\beta)} \|\beta\|^2 \left[\frac{1}{\|\beta\|^2} \sum_{j=1}^p \left(\sum_{i=1}^K \frac{x_{ij}e^{-x_i\beta}}{1+e^{-x_i\beta}} \right)^2 + 1 + \frac{1}{\|\beta\|^2} \sum_{j=1}^p \left(\sum_{i=1}^K (1-y_i)x_{ij} \right)^2 \right. \\ &\quad \left. + 2 \sum_{i=1}^K (1-y_i) \frac{x_i\beta}{\|\beta\|^2} - 2 \sum_{i=1}^K \frac{x_i\beta}{\|\beta\|^2} \frac{e^{-x_i\beta}}{1+e^{-x_i\beta}} \right. \\ &\quad \left. - 2 \frac{1}{\|\beta\|^2} \sum_{j=1}^p \left(\sum_{i=1}^K (1-y_i)x_i \right) \left(\sum_{i=1}^K x_{ij} \frac{e^{-x_i\beta}}{1+e^{-x_i\beta}} \right) \right] \end{aligned}$$

and

$$\begin{aligned}
& \frac{\|\nabla f(\beta)\|^2}{e^{2C(\beta)}\|\beta\|^2} \\
&= \frac{1}{\|\beta\|} \left[\frac{1}{\|\beta\|} \sum_{j=1}^p \left(\sum_{i=1}^K \frac{x_{ij} e^{-x_i \beta}}{1 + e^{-x_i \beta}} \right)^2 + \frac{1}{\|\beta\|} \sum_{j=1}^p \left(\sum_{i=1}^K (1 - y_i) x_{ij} \right)^2 + 2 \sum_{i=1}^K (1 - y_i) \frac{x_i \beta}{\|\beta\|} \right. \\
&\quad \left. - 2 \sum_{i=1}^K \frac{x_i \beta}{\|\beta\|} \frac{e^{-x_i \beta}}{1 + e^{-x_i \beta}} - 2 \frac{1}{\|\beta\|} \sum_{j=1}^p \left(\sum_{i=1}^K (1 - y_i) x_i \right) \left(\sum_{i=1}^K x_{ij} \frac{e^{-x_i \beta}}{1 + e^{-x_i \beta}} \right) \right] + 1. \quad (36)
\end{aligned}$$

Since $\lim_{\|\beta\| \rightarrow \infty} \|\beta\|^{-1} \rightarrow 0$, it is left to show that the term in the square brackets is bounded in the limit. Since y_i and x_{ij} are independent of β , and $e^{-x_i \beta}/(1 + e^{-x_i \beta})$ bounded below by 0 and above by 1, it is only required to show that the third and fourth terms in the square brackets remain bounded in the limit. From (35) and the Cauchy-Schwarz inequality

$$- \sum_{i=1}^K (1 - y_i) \|x_i\|_1 \leq 2 \lim_{\|\beta\| \rightarrow \infty} \sum_{i=1}^K (1 - y_i) \frac{x_i \beta}{\|\beta\|} \leq 2 \sum_{i=1}^K (1 - y_i) |x_i|.$$

In addition,

$$\begin{aligned}
\sum_{i=1}^K \frac{x_i \beta}{\|\beta\|^2} \frac{e^{-x_i \beta}}{1 + e^{-x_i \beta}} &\geq - \sum_{i=1}^K \sum_{j=1}^p \frac{|x_{ij}| |\beta_j|}{\|\beta\|} \frac{e^{-x_i \beta}}{1 + e^{-x_i \beta}} \\
&\geq - \sum_{i=1}^K \sum_{j=1}^p \frac{|x_{ij}| |\beta_j|}{\|\beta\|} \\
&\geq - \sum_{i=1}^K \|x_i\|_1.
\end{aligned}$$

Thus, by the above result and (34),

$$- \sum_{i=1}^K \|x_i\|_1 \leq \lim_{\|\beta\| \rightarrow \infty} \sum_{i=1}^K \frac{x_i \beta}{\|\beta\|} \frac{e^{-x_i \beta}}{1 + e^{-x_i \beta}} \leq \sum_{i=1}^K |x_i|.$$

Using these results in (36),

$$\begin{aligned}
& \lim_{\|\beta\| \rightarrow \infty} \frac{\|\nabla f(\beta)\|^2}{e^{2C(\beta)} \|\beta\|^2} \\
&= 1 + \lim_{\|\beta\| \rightarrow \infty} \frac{1}{\|\beta\|} \left[\frac{1}{\|\beta\|} \sum_{j=1}^p \left(\sum_{i=1}^K \frac{x_{ij} e^{-x_i \beta}}{1 + e^{-x_i \beta}} \right)^2 + \frac{1}{\|\beta\|} \sum_{j=1}^p \left(\sum_{i=1}^K (1 - y_i) x_{ij} \right)^2 \right. \\
&\quad + 2 \sum_{i=1}^K (1 - y_i) \frac{x_i \beta}{\|\beta\|} - 2 \sum_{i=1}^K \frac{x_i \beta}{\|\beta\|} \frac{e^{-x_i \beta}}{1 + e^{-x_i \beta}} \\
&\quad \left. - 2 \frac{1}{\|\beta\|} \sum_{j=1}^p \left(\sum_{i=1}^K (1 - y_i) x_i \right) \left(\sum_{i=1}^K x_{ij} \frac{e^{-x_i \beta}}{1 + e^{-x_i \beta}} \right) \right] \\
&= 1.
\end{aligned}$$

Next observe that

$$\begin{aligned}
\beta \cdot \nabla f(\beta) &= e^{C(\beta)} \sum_{j=1}^p \left[-\beta_j^2 - \sum_{i=1}^K (1 - y_i) x_{ij} \beta_j + \sum_{i=1}^K x_{ij} \beta_j \frac{e^{-x_i \beta}}{1 + e^{-x_i \beta}} \right] \\
&= e^{C(\beta)} \left[-\|\beta\|^2 - \sum_{i=1}^K (1 - y_i) x_i \beta + \sum_{i=1}^K x_i \beta \frac{e^{-x_i \beta}}{1 + e^{-x_i \beta}} \right].
\end{aligned}$$

and hence

$$\frac{\beta \cdot \nabla f(\beta)}{\|\beta\| \|\nabla f(\beta)\|} = \frac{e^{C(\beta)}}{\|\nabla f(\beta)\|} \left[-\|\beta\| - \sum_{i=1}^K (1 - y_i) \frac{x_i \beta}{\|\beta\|} + \sum_{i=1}^K \frac{x_i \beta}{\|\beta\|} \frac{e^{-x_i \beta}}{1 + e^{-x_i \beta}} \right].$$

We conclude that

$$\begin{aligned}
\lim_{\|\beta\| \rightarrow \infty} \frac{\beta \cdot \nabla f(\beta)}{\|\beta\| \|\nabla f(\beta)\|} &= \lim_{\|\beta\| \rightarrow \infty} \frac{e^{C(\beta)} \|\beta\|}{\|\nabla f(\beta)\|} \left[-1 - \sum_{i=1}^K (1 - y_i) \frac{x_i \beta}{\|\beta\|^2} + \sum_{i=1}^K \frac{x_i \beta}{\|\beta\|^2} \frac{e^{-x_i \beta}}{1 + e^{-x_i \beta}} \right] \\
&= -1
\end{aligned}$$

which establishes (32). \square

E Univariate Termination Rules

In this section we formally present the univariate termination rules we implement in Section 5 of the main document. Recall that for the i th component of θ , $\theta_{n,i}$ is the Monte Carlo estimate for θ_i , and σ_i^2 is the asymptotic variance in the univariate CLT. Let $\sigma_{n,i}^2$ be the univariate batch means estimator of σ_i^2 and let $\lambda_{n,i}^2$ be the sample variance for the i th component.

Common practice is to terminate simulation when *all* components satisfy a termination rule. We focus on the relative standard deviation fixed-width sequential stopping rules. Due to multiple testing, a Bonferroni correction is often used. We will refer to the uncorrected method as the uBM method and the corrected method as the uBM-Bonferroni. To create $100(1 - \alpha)\%$ univariate confidence intervals, the relative standard deviation fixed-width rule terminates at the random time,

$$\inf \left\{ n \geq 0 : \frac{1}{\lambda_{n,i}} \left(2t_* \frac{\sigma_{n,i}}{\sqrt{n}} + \epsilon_i \lambda_{n,i} I(n < n^*) + \frac{1}{n} \right) \leq \epsilon_i \text{ for all } i = 1, \dots, p \right\},$$

where for uncorrected intervals $t_* = t_{1-\alpha/2, a_n-1}$ and for Bonferroni corrected intervals $t_* = t_{1-\alpha/2p, a_n-1}$. See Flegal and Gong (2015) for more details.

Remark 8. If it is unclear which features of F are of interest *a priori*, i.e., g is not known before simulation, one can implement Scheffe's simultaneous confidence intervals. This method can also be used to create univariate confidence intervals for arbitrary contrasts *a posteriori*. Scheffe's simultaneous intervals are boxes on the coordinate axes that bound the confidence ellipsoids. For all $a^T \theta$, where $a \in \mathbb{R}^p$,

$$a^T \theta_n \pm \sqrt{a^T \Sigma_n a \frac{p(a_n - 1)}{(a_n - p)} F_{1-\alpha, p, a_n - p}}$$

will have simultaneous coverage probability $1 - \alpha$. Since we generally are not interested in all possible linear combinations, Scheffe's intervals are often too conservative. In

fact, if the number of confidence intervals is less than p , Scheffe’s intervals are more conservative than Bonferroni corrected intervals.

F Computational Cost

The multivariate termination rule is naturally more expensive than the univariate termination rule, but in our experience, the time to check the termination criterion is insignificant compared to the time it takes for obtaining more samples. Also note that there are cases when it is almost impossible to meet the termination criterion in machine time using univariate methods. This was demonstrated for the Bayesian dynamic spatial-temporal example.

We present computational time to termination for the Bayesian logistic and the VAR(1) models. For the VAR(1) model, we keep the eigen-structure for Φ as the same as in Section 5.2 of the main document, but let $p = 50$. Samples from both of the MCMC processes are obtained fairly quickly due to the inexpensive structure. Calculating the multivariate estimators for the VAR(1) model will take more time since we are estimating a 50×50 matrix. However, since one component mixes slowly, termination by univariate methods is delayed.

In Table 8 we present mean computational time to termination using mBM and uBM-Bonferroni over 100 replications for two values of the precision ϵ (we make 90% confidence regions). Time to termination is significantly lower for mBM methods, although the difference might not be practically significant. It is important to note that in the Bayesian logistic regression sampler, all the components seem to be mixing equally, so termination is not delayed due to that reason.

In Table 9 we present mean computational time to termination for the VAR(1) model with $p = 50$ over 100 replications. Here, the Bonferroni correction and one slow mixing component both lead to delayed univariate termination, and large p causes mBM

Table 8: Bayesian Logistic: Computation time in seconds for termination using multivariate and univariate techniques. $b_n = \lfloor n^{1/2} \rfloor$.

	mBM	uBM-Bonferroni
$\epsilon = .02$	42.16 (0.308)	43.30 (0.327)
$\epsilon = .01$	161.83 (0.708)	165.18 (0.731)

calculation to be slower than univariate methods. However, we see significant gains in computational time using multivariate termination rules.

Table 9: VAR(1): Computation time in seconds for termination using multivariate and univariate techniques. $b_n = \lfloor n^{1/3} \rfloor$.

	mBM	uBM-Bonferroni
$\epsilon = .02$	40.56 (0.044)	58.11 (0.061)
$\epsilon = .01$	172.91 (0.826)	251.04 (1.477)

Both these examples were in a way best case scenario for the univariate methods because obtaining samples is cheap for both examples. Even then we see multivariate termination methods require less computation time for the same level of precision ϵ .

G Sensitivity to Batch Size

We explore the finite sample properties of using large and small batch sizes for the VAR example. Table 10 has coverage probabilities over 1000 replications for different choices of tolerance level ϵ in the relative volume sequential stopping rule. Generally a smaller ϵ is chosen so as to ensure reasonable coverage probabilities.

The difference in the coverage probabilities is minimal for $\epsilon \leq .05$ between the three batch sizes. Although, for larger ϵ , the batch size has a greater impact. However, for large batch sizes, the variability in the estimation of Σ is larger since less number of batches are available for estimation. Figure 5 shows the estimated density of the largest estimated eigenvalue over 1000 replications. Thus, for large batch sizes, the estimation is

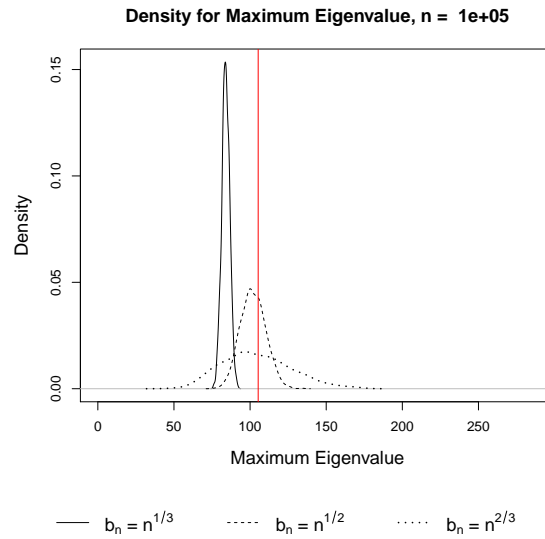


Figure 5: Var: Replications = 1000. Density of the largest estimated eigenvalue of Σ using mBM estimator for three batch sizes.

less biased, however, the variability in the estimates is considerably larger. The opposite phenomenon is witnessed for small batch sizes. But since the Monte Carlo sample size is large enough, the batch size of $b_n = \lfloor n^{1/2} \rfloor$ has low bias and low variability.

Table 10: VAR Example. Coverage probability of 90% confidence regions using mBM. Replications = 1000. $n^* = 1000$.

b_n, ϵ	0.20	0.10	0.05	0.02	0.01
$\lfloor n^{1/3} \rfloor$	0.812 (0.0124)	0.869 (0.0107)	0.886 (0.0101)	0.883 (0.0102)	0.900 (0.0095)
$\lfloor n^{1/2} \rfloor$	0.884 (0.0101)	0.898 (0.0096)	0.911 (0.0090)	0.894 (0.0097)	0.909 (0.0091)
$\lfloor n^{2/3} \rfloor$	0.877 (0.0104)	0.905 (0.0093)	0.912 (0.0090)	0.894 (0.0097)	0.904 (0.0093)